CONSTRAINTS ON DEVELOPMENT OF ANOXIA THROUGH GEOCHEMICAL FACIES MAPPING OF DEVONIAN BLACK SHALES IN THE MIDCONTINENT

By

ROBERT RITER BERRYMAN

Bachelor of Science in Geology

Oklahoma State University

Stillwater, OK

2008

Submitted to the Faculty of the
Graduate College of the
Oklahoma State University
in partial fulfillment of
the requirements for
the Degree of
MASTER OF SCIENCE
May, 2012

CONSTRAINTS ON DEVELOPMENT OF ANOXIA THROUGH GEOCHEMICAL FACIES MAPPING OF DEVONIAN BLACK SHALES IN THE MIDCONTINENT

Thesis Approved:

Dr. Jim Puckette

Thesis Adviser

Dr. Darwin Boardman

Dr. Anna Cruse

Dr. Sheryl Tucker

Dean of the Graduate College

.

TABLE OF CONTENTS

LIST OF TABLES

Table Page

LIST OF FIGURES

Figure Page

CHAPTER I

INTRODUCTION

The Woodford Shale is a prolific hydrocarbon-source rock throughout the southern Midcontinent of the United States as well as in south-central Oklahoma where it produces both oil and gas (Comer, 2005). The Woodford Shale is a highly radioactive, carbonaceous and siliceous, dark gray to black shale and large areas of the Woodford have attained the maturation levels required for hydrocarbon generation (Hester et al, 1990). Although it is widely accepted that the Woodford Shale was deposited under generally anoxic conditions (Comer, 2005; Kirkland et al., 1992; Romero and Philp, 2011), there is little understanding about the details concerning redox conditions at the time of deposition such as geographic extent and temporal persistence of anoxic conditions. The purpose of this study is to conduct trace element analysis and percent of total organic carbon (TOC) from outcrops of the Woodford Shale to better constrain the development of anoxia at the time of deposition.

Redox sensitive trace element concentrations are among the most widely used indicators of redox conditions in modern and ancient sedimentary systems (Algeo and Maynard, 2004; Calvert and Pederson, 1993; Cruisus et al., 1996). Trace elements

.

commonly exhibit considerable enrichment in laminated, organic rich facies, especially those deposited under euxinic conditions (Algeo and Maynard, 2004). The hypothesis is that trace metal/TOC geochemical analysis can determine the redox conditions which will provide further evidence concerning bottom water conditions during deposition, which can be used in interpretations of environmental conditions such as water column depth and surface water productivity. These interpretations are important in the development of refined depositional models for oil and gas producing shales to aid in exploration.

CHAPTER II

BACKGROUND

The study area is located in the Ardmore Basin, which is a sedimentary basin located in south central Oklahoma (Figure 1). Crustal extension occurred in the southern Oklahoma aulacogen as late as the Cambrian and this event produced normal faults and emplaced igneous rocks in the region (Cardott and Lambert, 1985). Subsidence, in several phases, occurred in the aulacogen from Late Cambrian through Early Mississippian and is ascribed to cooling after a thermal event associated with Cambrian crustal thinning (Cardott et al., 1985). Uplift and erosion during the Early Devonian is marked by a major unconformity below the Woodford Shale (Cardott and Lambert, 1985). The Acadian Orogeny began at the end of the Devonian during the deposition of the Woodford Shale. Following the Acadian Uplift there was another period of deposition occurring between the Devonian and the Early Pennsylvanian (Allen, 2000). The Criner Hills and the Pauls Valley Uplift formed during the Wichita Orogeny which was followed by another period of deposition. In the Late Pennsylvanian, the Arbuckle Orogeny formed the Caddo Anticline and the Arbuckle Mountains (Allen, 2000), (Figure 2).

Late Ordovician, Silurian, and Early Devonian strata with similar lithofacies-

biofacies characteristics can be traced over a wide area in the southern Midcontinent region, indicating the presence of a large, shallow, epicontinental carbonate basin, or a series of interconnected basins (Amsden, 1989). The distribution of organic-rich Woodford Shale facies is the result of Late Devonian paleogeography (Figure 3) , when the southern Mid-continent lay along the western margin of North America in the warm dry tropics near 15° south latitude (Comer, 2005).

Taft (1903) named and described the Woodford Shale at the type locality located in Carter County, Oklahoma. The Woodford Shale (Upper Devonian-Lower Mississippian), originally known as an oil source rock with type II kerogen, has become an important gas shale in the last decade (Cardott, 2005). Time-stratigraphic equivalents of the Woodford Shale include the New Albany, Chattanooga, Bakken, Ohio, Millboro, Burket, Geneseo, Antrim Shales, and the Arkansas Novaculite (Cardott and Lambert, 1985; Lambert 1993).

The predominant lithology for the Woodford is black shale, but it also includes chert, siltstone, sandstone, dolostone, and light colored shale (Comer, 2005; Amsden, 1975). The Woodford Shale is thought to have been deposited in generally anoxic conditions during the Kaskaskian marine transgression on a major regional unconformity developed in the Late Devonian (Amsden, 1975; Lambert, 1993). The Woodford Shale is unconformably overlain by shales and limestones of Early Mississippian (Kinderhookian) age (Hester et. al, 1990), (Figure 4). Woodford deposition began as sea level rose and began to flood marine embayments in what are today the deepest parts of the Delaware, Val Verde, Anadarko, and Arkoma Basins and advanced over subaerially eroded terrane of mostly Ordovician to Middle Devonian carbonate rocks (Comer, 2005). Total

thickness ranges from near zero to about 125 feet (40 m) on the extensive northern shelf areas and increases to more than 900 feet (270 m) in limited parts of the deep Anadarko Basin (Amsden, 1975; Hester et al., 1990). Kirkland et al. (1992) restored the depositional thickness of the Woodford (Figure 5). The Woodford is carbonaceous and siliceous as well as highly radioactive dark-gray to black shale.

Conodont biostratigraphy data from Amsden and Klapper (1972) was used to date the basal Misener Sandstone of the Woodford Shale in north-central Oklahoma as Middle to Late Devonian (Givetian to early Famennian) in age. Hass and Huddle (1965) also conducted conodont biostratigraphy to determine the age of the upper Woodford Shale in south-central Oklahoma to be mostly Late Devonian (Famennian) and the uppermost 2 feet to be Early Mississippian (Kinderhookian).

Using geophysical logs, Ellison (1950) and Comer (1991), distinguished three shale units within the Woodford Shale of the Permian Basin and Hester et al. (1988) found the same three units in the Woodford of northwestern Oklahoma and informally named them the lower, middle, and upper shale members (Lambert, 1993). Hester et al. (1990) uses the kerogen content of the middle member as the physical basis for subdivision and in terms of wire-line character, the Woodford Shale can be generally described as two similar shales separated by a less dense, more radioactive, and more resistive middle member.

STUDY AREA

Two outcrops were chosen for this project, the McAlister Shale Pit (MSP) and an outcrop located on Oklahoma State Highway 77D, refer to figure 1 in the geologic background section. The McAlister Shale Pit (MSP) is located in south Carter County,

Oklahoma, SW1/4, Sec. 36 T.5S., R1E (latitude N 34°04.868 longitude W 97°09.395), elevation ~846 ft. The highway 77D outcrop is located in central Murray County, Oklahoma, NE 1/4, Sec. 30 T1S., R2E, latitude N 34°26.699 longitude W 97°07.849, elevation ~850 ft.

McAlister Shale Pit (MSP)

This outcrop consists of a complete section of Woodford Shale (~ 325 ft.). At this location the Woodford is exposed on a faulted asymmetrical anticline. The beds consisted of mostly black siliceous shale that varied in fissility and brittleness. The Woodford Shale beds at this location are dipping 35º to the northeast (Figure 6). The bleached upper Woodford Shale is folded and faulted and contains abundant phosphate nodules and chert in the high wall at the McAlister Shale Pit (Figure 7). Samples were taken at 1.75 ft. intervals.

Highway 77D Outcrop.

Outcrop 77D is located 25 miles north of McAlister Shale Pit and approximately one mile north of Washita Fault. The Woodford here is also characterized by alternating fissile and silica-rich beds (Figure 8). Highway 77D outcrop shows the lower contact of Woodford Shale and underlying Hunton Group. It has a sandy glauconitic zone at base (Figure 9). This likely reflects deposition under a shallower water column than at McAlister Shale Pit.

MECHANISMS FOR BLACK SHALE FORMATION

Black shales are usually interpreted as relatively deep water facies that form in basin center locations in epicontinental settings (Wignall and Maynard, 1993). Modern analogues for black-shale forming environments have been studied to determine the nature and position of the redox boundary and its effect on benthic communities. Redox describes the extent of oxygenation of the water column, with 'oxic' meaning dissolved oxygen is present. Anoxic means no dissolved oxygen is present. Euxinic means that no dissolved oxygen is present and free dissolved sulfide exists in the water column. The redox state is controlled by the extent of organic matter degradation; degradation of organic matter (OM) consumes oxygen, and if the dissolved oxygen is not renewed by turnover, then water column will become anoxic.

The principal controls on the accumulation of organic carbon in marine sediments include bulk sediment accumulation rate, water column anoxia, and the rate of supply of organic matter to the sea floor (Demaison and Moore, 1980). In such relatively deep waters of epicontinental seas settings, the benthic environment can be poorly oxygenated (anoxic or dysoxic) due to isolation of the bottom waters from effects such as the wind driven vertical advection of oxygen rich surface waters. The establishment of a pycnocline can further isolate bottom waters, enhancing the development of anoxic/euxinic conditions (Wignall and Maynard, 1993). Anoxia in the water column arises from the complex interplay of (1) restricted lateral circulation in the deep water column, (2) thermohaline stratification, and (3) levels of primary productivity and export of organic carbon from the surface waters, such that respiratory oxygen demand in lower levels of the water column exceeds renewal (Cruse and Lyons, 2004). While

considerable debate still exists regarding the ultimate driving mechanisms behind the deposition of organic-rich mudstones, two first-order tectonic and/or climatic controls on their occurrence are 1) the existence of sediment accommodation, and 2) the existence of persistent or at least intermittent bottom water anoxia (Rowe et al., 2008). Betts and Holland (1991) have conducted studies that they believe are conclusive that the primary control of the burial efficiency of organic matter in marine sediments is the sedimentation rate. Demaison and Moore (1980) have suggested that bottom water anoxia or low oxygen concentrations enhance long term carbon preservation in sediments. Pedersen and Calvert (1990) suggest that high primary production and not water column anoxia provides first order control on the accumulation of organic rich facies in the modern oceans. Tyson 2001 concluded that the role of dissolved oxygen is likely dependent upon the sedimentation rate being considered and that under very slow deposition TOC will critically depend on the burial efficiency, which appears to be partly dependent on the dissolved oxygen.

Primary production of organic matter in the open ocean by a wide range of unicellular plankton is primarily controlled by nutrient supply and solar radiation (Pedersen and Calvert, 1990). The vast majority of primary production in the ocean is confined to the photic zone, where sufficient light is available for photosynthesis; the depth of this layer varies between ~30-100 m. Sustained levels of primary production are only possible when and where nutrients are resupplied to the surface layers, either from land runoff, groundwater flow, atmospheric deposition, or from the vertical movement and mixing of sub-surface waters in the surface photic layer (Piper and Calvert, 2009).

A global average of less than 20% of the organic matter produced in the surface waters escapes consumption/oxidation within the photic zone, of that material 75-85% is decomposed further (Arthur, 1994). Only a fraction of the organic matter produced in the euphotic zone is exported and settles into deeper water, part of this material is oxidized during settling, part is used as food by benthic organisms, part undergoes further degradation in the sediment, and the remainder is buried (Pedersen and Calvert, 1990). Concentrations of organic matter in sediments and sedimentary rocks record only a fraction of the total biological productivity in surface waters of the ocean (Tribovillard et al., 2006).

Elemental Indicators of Depositional Environment

Trace metals have long been used as proxies, or indirect indicators, of water column redox conditions during deposition and /or diagenesis. Trace metals may also be used to infer water-column or pore- water oxygen levels, original organic matter flux, and water column productivity (Figure 10; Calvert and Pedersen, 1993; Piper and Calvert, 2009; Tribovillard et al., 2006). The use of trace metals as redox proxies results from the different valence states in which these elements can exist at surface temperatures' and pressures. Further, the solubility and reactivity of such elements changes with valence state. For example, under oxic conditions Fe is present in the +3 state and it precipitates as an oxide mineral. If anoxic conditions are established, Fe^{+3} are reduced to Fe^{+2}, which do not form oxide minerals. Hence, any iron oxides present in the sediments or as particles in the water column are dissolved, releasing dissolved Fe to the water column. However, Fe^{+2} rapidly form pyrite if any S^{-} is present.

The reduced forms of other metals, such as V or U will be fixed in sediments by other mechanisms, such as scavenging by OM, but those reactions only occur when the metal is in its reduced state. Ni, Cu, and Mo are scavenged by organic matter under suboxic (Ni, Cu) to euxinic (Mo) conditions. Some of these redox-sensitive elements (Ni, Cu, Zn, Cd) are delivered to the sediment mainly in association with organic matter and they may be retained within the sediment in association with pyrite. This mechanism makes Ni and Cu good proxies for productivity (Tribovillard et al., 2006). Thus, ultimately, this leads to enrichments of trace metals in sediments during anoxic/euxinic conditions which are the same conditions that lead to the preservation of OM in sediments—which will become shale. During diagenetic and catagenic processes, OM can be lost, but the metals can be retained in the sediments. Under these conditions, enrichments in metals will not be well-correlated with TOC concentrations.

The bulk transition metal concentrations are a mix of both detrital and authigenic components, it is only the concentrations of the authigenic component that vary in response to changes in water-column redox conditions (Figure 11; Cruse and Lyons, 2004). Also, sediments and sedimentary rocks have variable proportions of mineral phases that may dilute the trace metal abundance of a sample. Thus, to be able to compare element proportions in samples it is customary to normalize trace element concentrations to the aluminum concentration; this is assumed to be only detrital in origin (Tribovillard et al., 2006). Metal/Al ratios can then be compared to a standard; the Post-Archean Average Shale (PAAS; Taylor and McLennan, 1985).

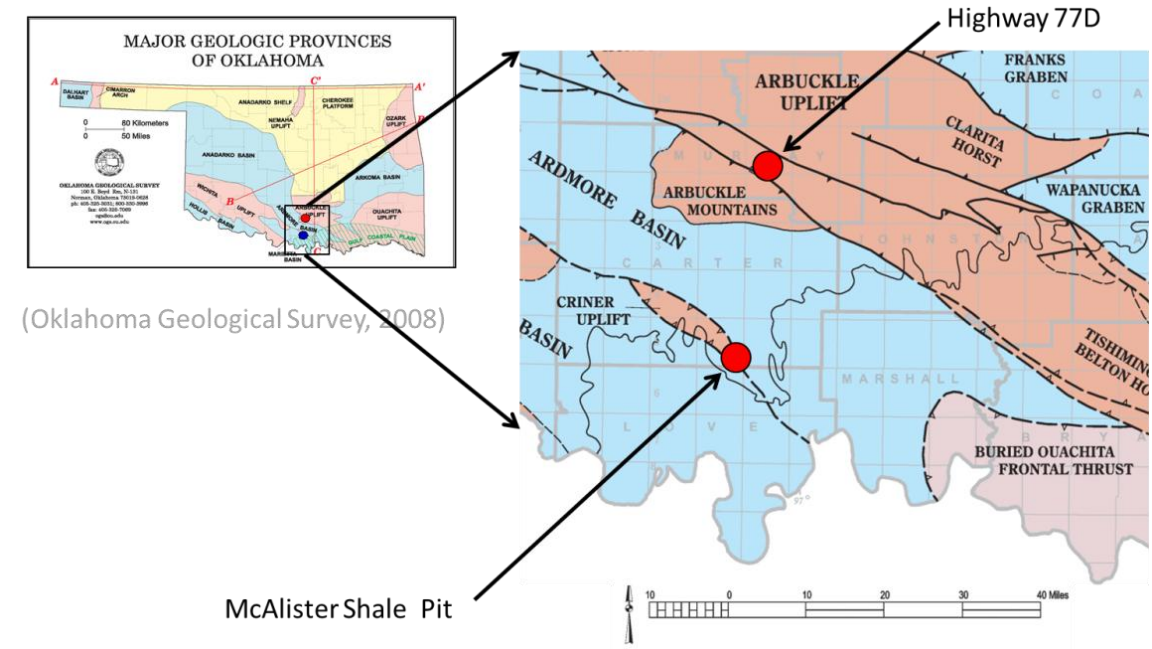

Figure 1. Location of study area in relation to Ardmore Basin, red circles represent the locations of the outcrops. The blue shading represent the deep basins, the lavender represents the detachment uplift, and the pink color represent basement-rooted uplift (Oklahoma Geological Survey, compiled by R.A. Northcutt and J. A. Campbell, 1995). Scale Bar = 40 miles.

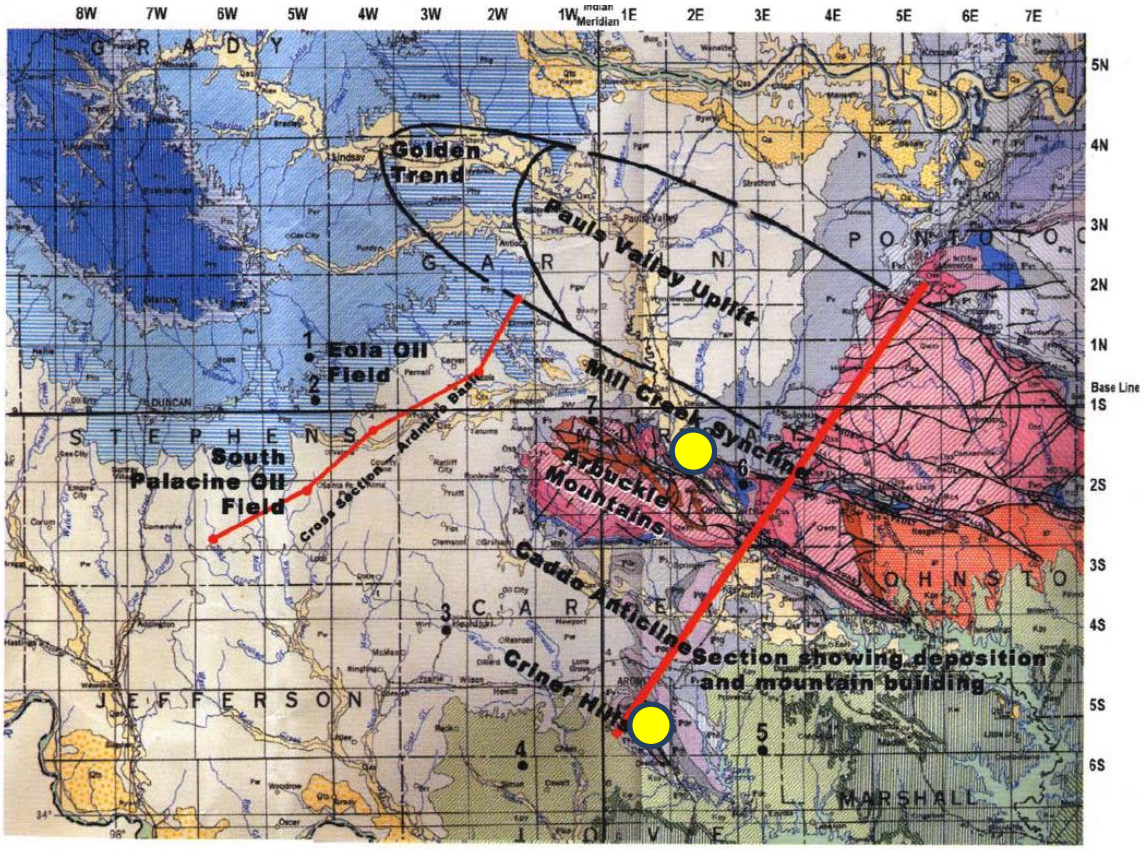

Figure 2. Map showing the location of the Arbuckle Mountains, Criner Hills, Pauls Valley Uplift, and the Caddo Anticline. Yellow dots indicate the location of study areas. The McAlister Shale pit is in the south, with 77D to the north (Allen, 2000).

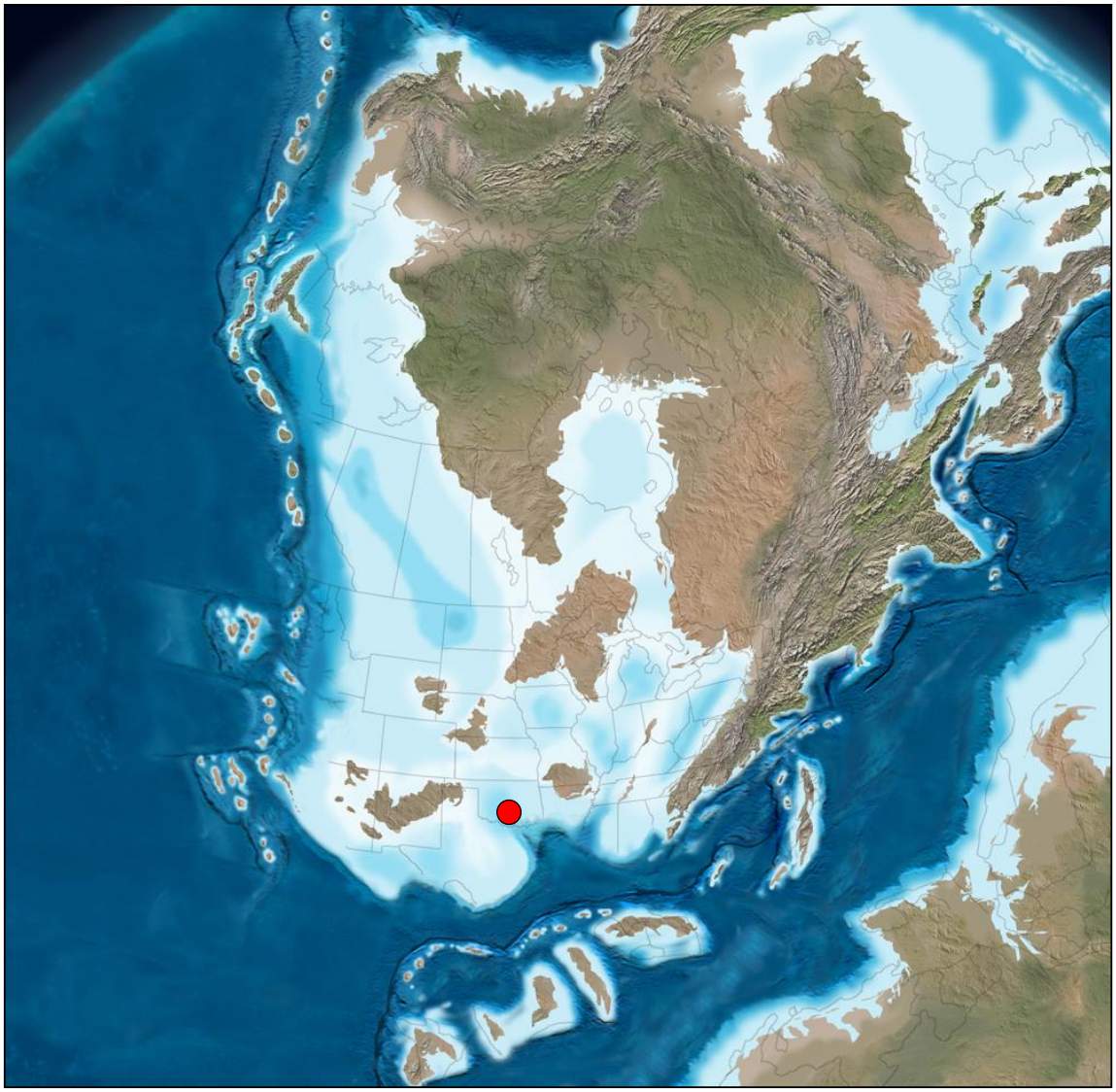

Figure 3. Paleogeographic map of the Late Devonian, red circle indicates the location of the study area. (Blakey, 2006).

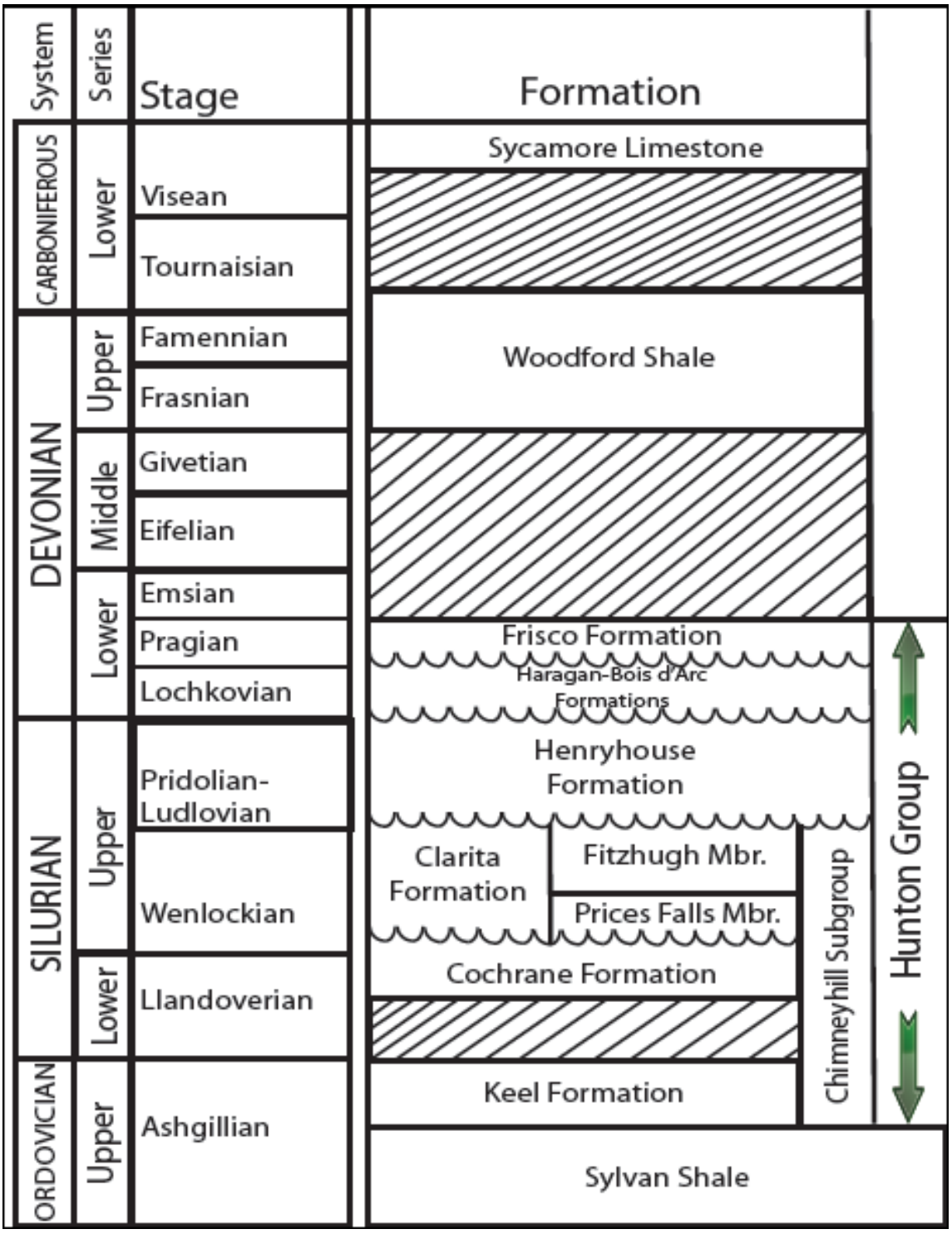

Figure 4. Generalized stratigraphic nomenclature for the study area, for the Upper Ordovician to Middle Mississippian strata in the Ardmore Basin (Boardman, 2011).

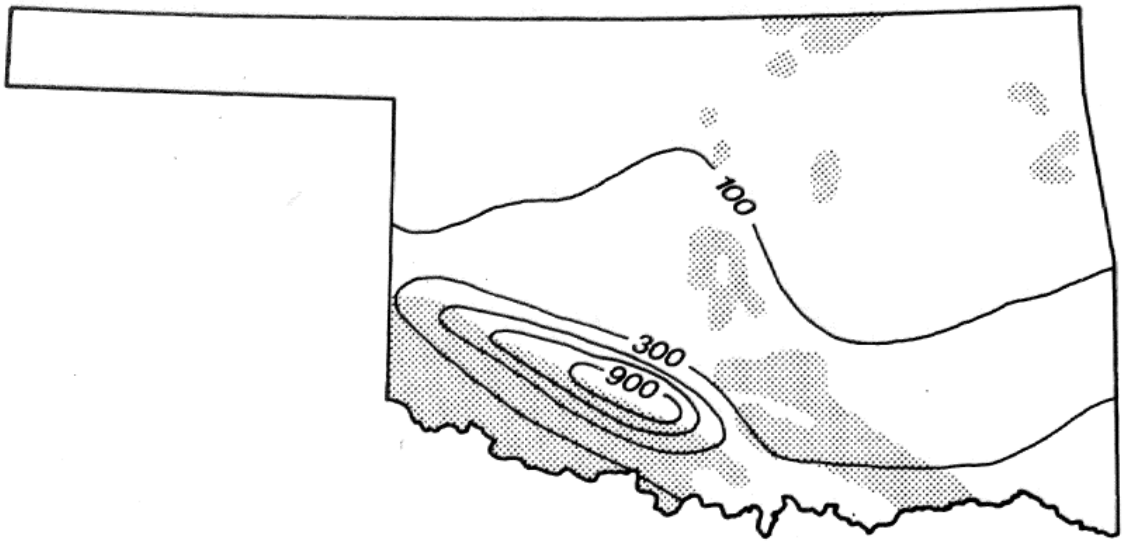

Figure 5. Restored depositional thickness map of the Woodford Shale, shading designates generalized areas from which the Woodford has been removed. Erosion, chiefly in the Late Paleozoic, removed the Woodford from parts of Oklahoma (Kirkland et al., 1992).

Figure 6. Carbonate concretions (not in place) resting on the eastward dipping middle section of the Woodford Shale at the MSP.

Figure 7. Folded and faulted bleached upper Woodford Shale with PO_4 and chert in the high wall at the McAlister Shale Pit.

Figure 8. Highway 77D outcrop showing the lower contact of Woodford Shale and the underlying Hunton Group.

Figure 9. Sandy glauconitic zone at the base of Woodford Shale at Highway 77D.

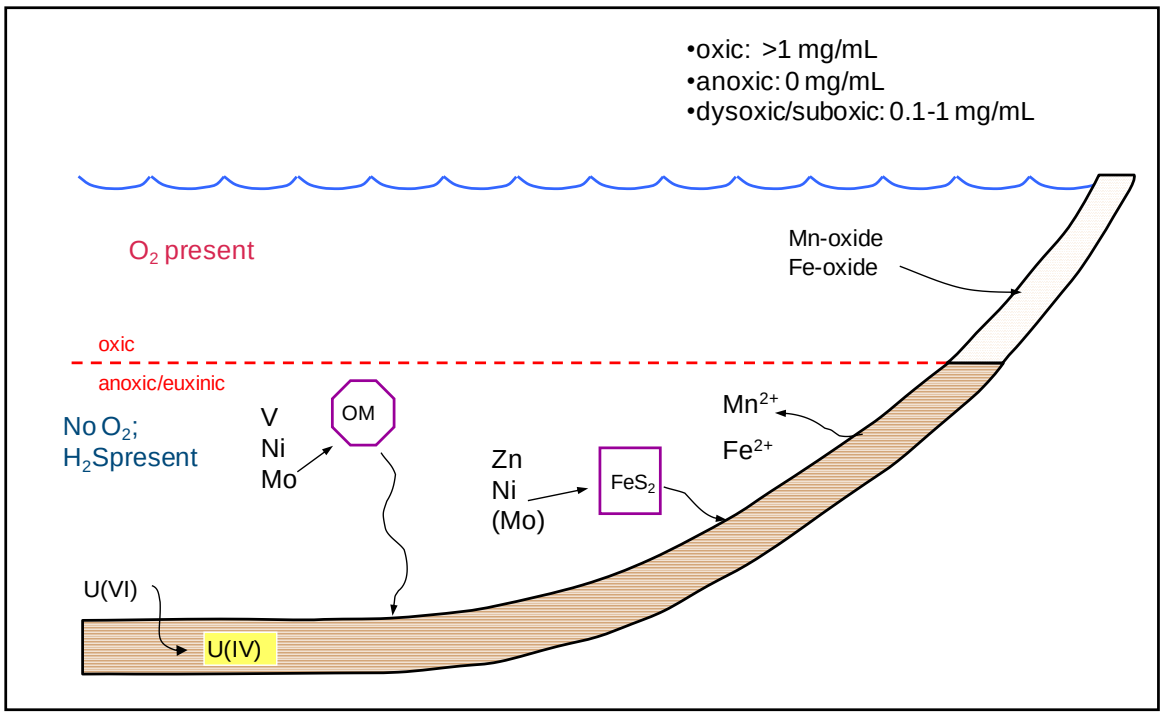

Figure 10. Schematic showing the relationships between organic matter, trace metals, and H_2S in sediments (Cruse, 2010).

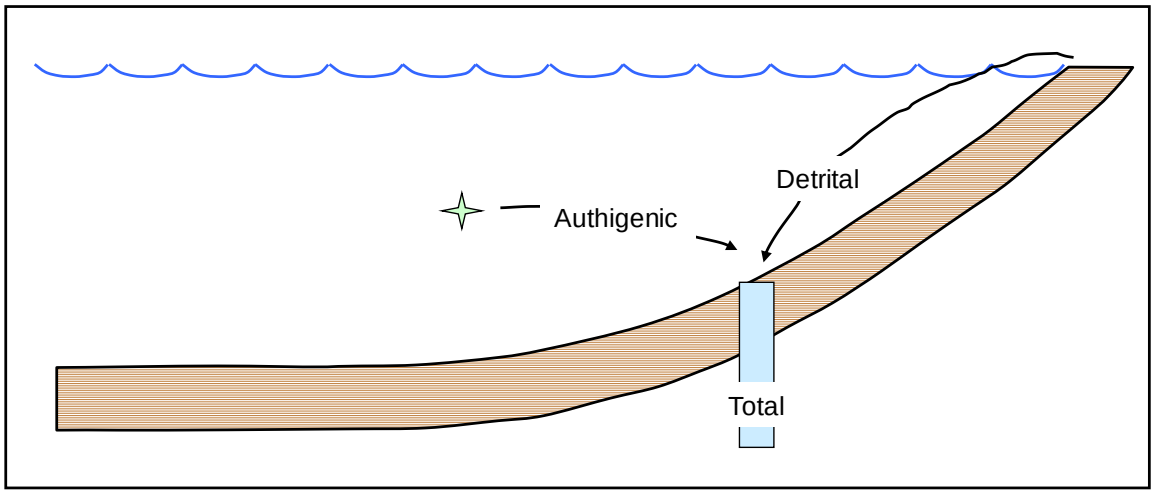

Figure 11. Schematic for the use of metal/Al ratios to determine the authigenic fraction of the total measured concentrations. From this, an authigenic concentration could also be calculated as: $[Me]_{auth} = [Me]_{total} - [Al]_{total}*[Me/Al]_{std}$. (Cruse, 2010).

CHAPTER III

METHODS

Powered samples were prepared from 119 samples collected from two outcrops in south central Oklahoma. Weathered material at both sample locations was removed to expose unweathered Woodford Shale (Figure 12). A total of 84 unweathered samples of Woodford Shale were collected from the McAlister Shale Pit beginning approximately 30 feet above the Woodford/Hunton contact. A total of 35 unweathered samples of Woodford Shale were collected from Highway 77D outcrop beginning at the base of the Woodford/Hunton contact (Figure 13). Samples at each location were collected at 1.75 foot stratigraphic intervals.

Samples were pulverized and powdered on the Spex Mill 8000, using an alumina ceramic ball and vial set. The powered samples were then prepared for laboratory analysis for trace metal and total organic carbon concentrations.

Total organic carbon (TOC) was determined by coulometric titration on the UIC Inc. CM 5014 CO_2 Coulometer (Figure 14). Total carbon concentrations were determined via combustion at 950°C on the UIC CM 5300 Furnace Apparatus. Total inorganic carbon concentrations values were determined via acidification with 2M $HClO_4$ on the UIC CM 5130 Acidification Module (Figure 14). Total organic carbon

concentrations were then determined by difference. Pure calcite was analyzed each day to ensure instrument stability. Calcite concentrations were measured within 95%. Measured concentrations of the calcite standards were used to correct measured sample concentrations for any instrumental inaccuracies.

Trace metal (Mo, Fe, U, Mn, V, Ni, Cu) concentrations were measured using the handheld Thermo Scientific Niton XL3t x-ray fluorescence analyzer (Figure 15; Tables 1 and 2). Sample plugs, weighing 4-5 grams, were prepared for use in the Thermo Scientific Niton test stand. The standard suite consisted of a comparison of three known standards: USGS SCo-1, PIC, and NIST 2780 standards. These standards were used to correct each measured concentration for any errors associated with matrix effects in the XRF. The measured concentrations from each standard were compared to the certified values. The differences between measured and certified values were used to calculate correction factors which were then applied to all analyses for a given day. Metal/Al ratios are presented relative to the Post-Archean Average Shale Standard (PAAS; Taylor and McLennan, 1985) in Table 3.

Figure 12. Sample sites from the McAlister Shale Pit (MSP), weathered material was removed to expose unweathered shale.

Figure 13. Woodford/Hunton contact at the outcrop located on Highway 77D.

Figure 14. The UIC CM 5014 CO_2 Coulometer (center), UIC CM 5300 Furnace Apparatus (right), and UIC CM 5130 Acidification Module (left).

Figure 15. Handheld Thermo Scientific Niton XL3t X-ray fluorescence analyzer (XRF).

CHAPTER IV

RESULTS

The samples from both outcrops were analyzed for the concentrations of a suite of trace elements and organic carbon was analyzed. The results from these analyses for select elements and organic carbon are presented graphically as depth plots for both outcrops (Figures 16 and 17). Generally speaking, as is expected for organic-rich mudrocks, these samples are generally enriched in the redox-sensitive elements and organic carbon, as compared to an average shale standard (PAAS). However, as is becoming evident, all mudrocks are not the same, and geochemical variations exist both with stratigraphic position in a given outcrop, as well as between outcrops.

The bulk transition metal concentrations are a mix of both detrital and authigenic components, it is only the concentrations of the authigenic component that vary in response to changes in water-column redox conditions (Cruse and Lyons, 2004). Also, sediments and sedimentary rocks have variable proportions of mineral phases that may dilute the trace metal abundance of a sample. Thus, to be able to compare element proportions in samples it is customary to normalize trace element concentrations to the

aluminum concentrations, this is assumed to be only detrital in origin (Tribovillard et al., 2006). Data is presented in plots of trace metal concentrations versus depth. Metal/Al ratios can then be compared to a standard; the Post-Archean Average Shale (PAAS; Taylor and McLennan, 1985), the ratio calculated for the PAAS (Table 3) is indicated by a dashed red line to provide an approximate baseline for the continental (detrital) mean.

TOTAL ORGANIC CARBON CONCENTRATIONS

Concentrations of organic carbon (TOC) of the Woodford Shale at the McAlister Shale Pit are greatly elevated with values ranging from 0.1-21.1 wt%, with an average of 12.9 wt% through the measured section. At depths from 30 to 110 feet there is a relatively wide range in variation in (TOC) concentrations compared to the up section samples. From 30 to 110 feet, the range in TOC concentrations is 3.8-20 wt. %, while the range for the samples above 110 ft. is only 9-21.1. However, above 110ft. there is an overall increase in TOC concentrations compared to the values observed below 110 ft. (Figure 16A).

Organic carbon concentrations for the Highway 77D outcrop are greatly elevated as well, with values ranging from 0.1-20.7 wt.%, with an average of 9.5 wt.% through the measured section. At 77D, from zero to 35 feet there is more variation of organic carbon concentrations with TOC ranging from 0.4-17.6 wt%. Above 35 feet there is less variation of organic carbon but the overall values decrease up section with TOC ranging from 3.9-13 wt% (Figure 17A).

TRACE METAL CONCENTRATIONS

Samples from McAlister Shale Pit as well as samples from 77D are enriched in all trace metals relative to the PAAS standard (Figures 16 and 17). However, the degree of enrichment is greater at the McAlister Shale Pit relative to 77D. For example, Fe/Al ratios at McAlister Shale Pit are, on average 4x higher than the ratio for PAAS. While at 77D is only an average of less than 2x the ratio for PAAS. At the McAlister Shale Pit there is a shift in trace metal behavior above 110 feet. Element concentrations (Mo, V, Cu, P, Ni, U, Fe) show less stratigraphic variation as well as decreasing values up section, while total sulfur concentrations (S) increase up section. Mn exhibits different behavior, however. Mn/Al ratios are less than PAAS from 40 to 115 ft. However, the Mn/Al ratios exhibit the same variation in concentrations with depth (less variation below 110 ft.; increased variation above 110 ft.).

Metal/Al ratios at 77D are enriched relative to PAAS but with only half the enrichment than at the McAlister Shale Pit. At 77D, there appears to be a shift of metal behavior at 26 feet, slightly below the depth at which TOC concentrations exhibit a shift in concentration variability. Metal concentrations (Fe, V, Ni) show less variation up section. (V, Ni, Cu) decreases up section as well as TOC and S. Uranium/Al ratios range between 42 and 174 throughout the outcrop, and show little systematic variations with depth. Phosphorus/Al ratios concentrations are generally less than the PAAS standard, but above 37 ft. increase up section (Figure 17). Mn/Al ratios exhibit extreme variation (0 to 73 ft), with most values generally below PAAS standard.

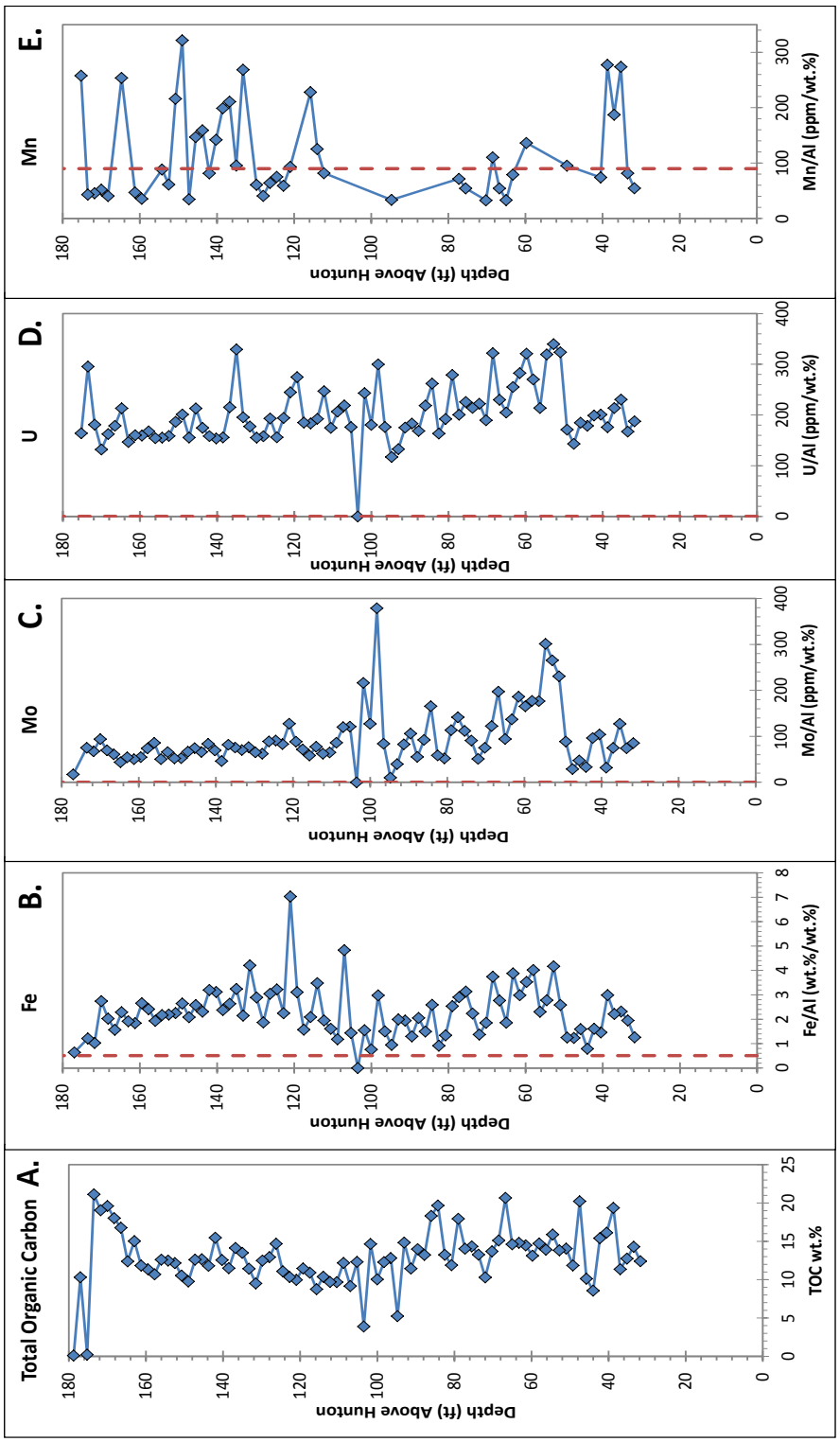

Figure 16. Aluminum normalized metal concentrations for the Woodford Shale from the McAlister Shale Pit: (A) TOC; (B) Fe/Al; (C) Mo/Al; (D) U/Al; and (E) Mn/Al versus depth above the Hunton Limestone. Dashed red lines represent the concentration ratio in the Post-Archean Average Shale (PAAS; Taylor and McClennan, 1985).

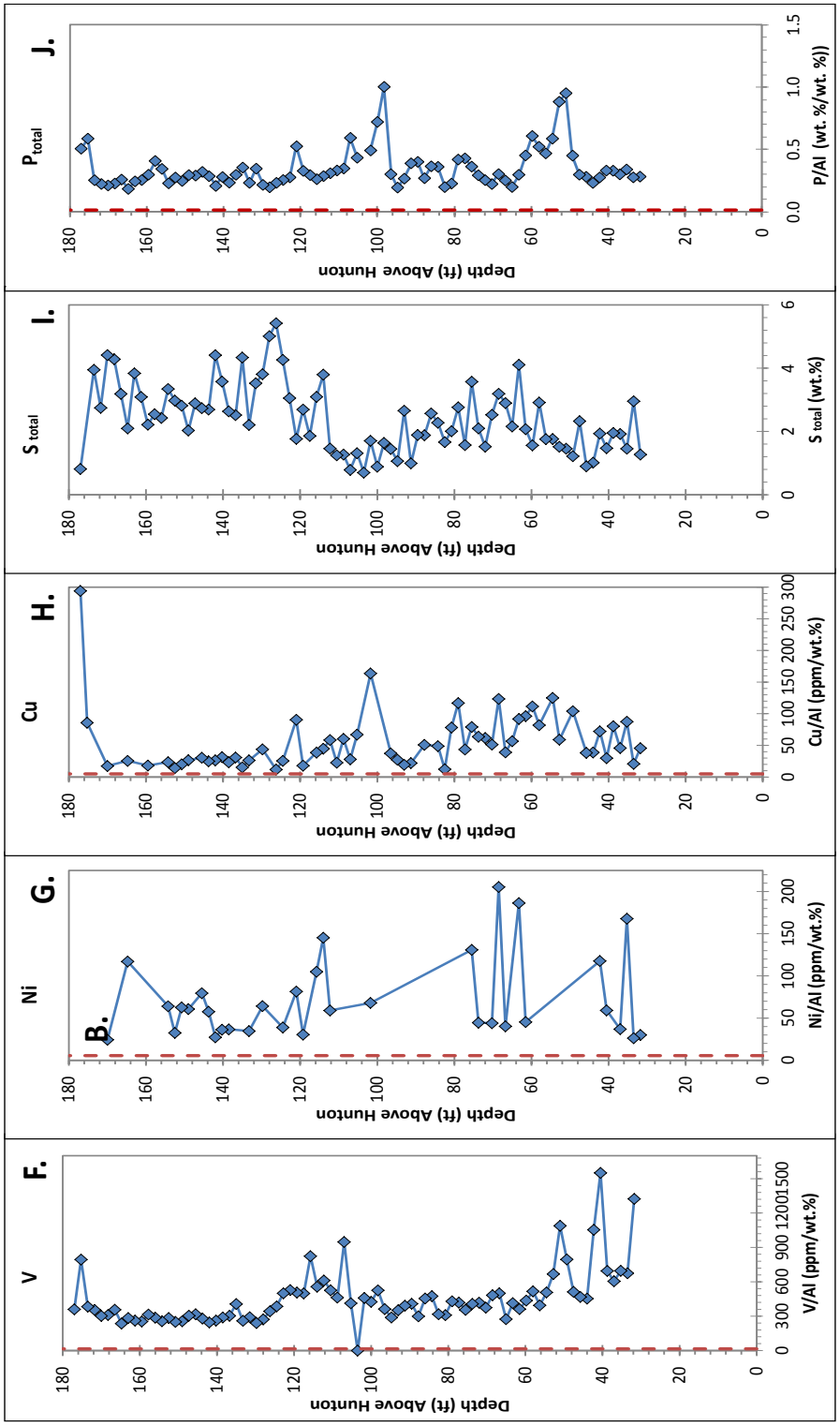

.

Figure 16 continued. (F) V/Al; (G) Ni/Al; (H) Cu/Al; (I) S/Al; and (J) P/Al.

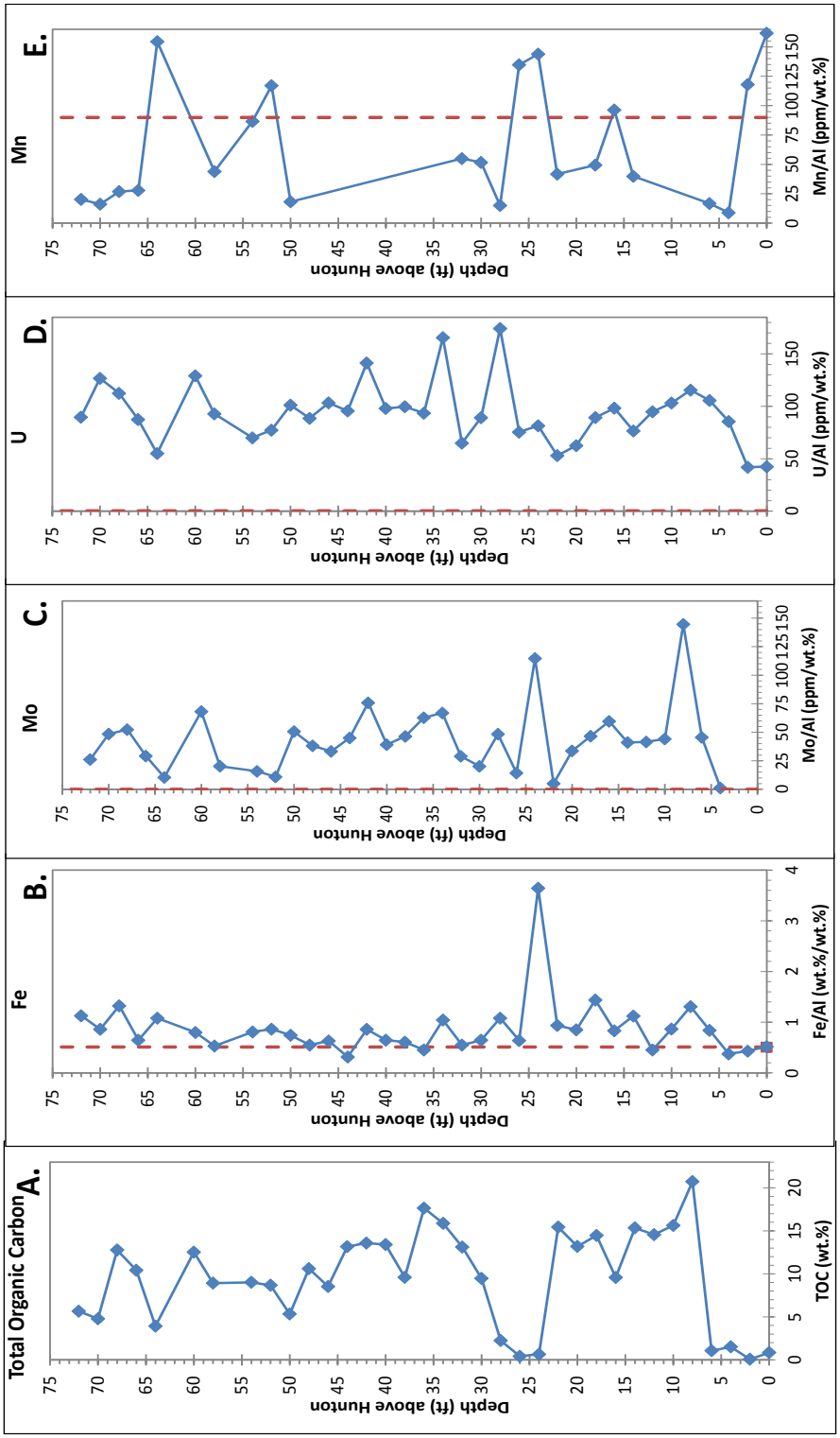

Figure 17. Aluminum normalized metal concentrations for the Woodford Shale from Highway 77D outcrop: (A) TOC; (B) Fe/Al; (C) Mo/Al; (D) U/Al; and (E) Mn/Al versus depth above the Hunton Limestone. Dashed red lines represent the concentration ratio in the Post-Archean Average Shale (PAAS; Taylor and McClennan, 1985).

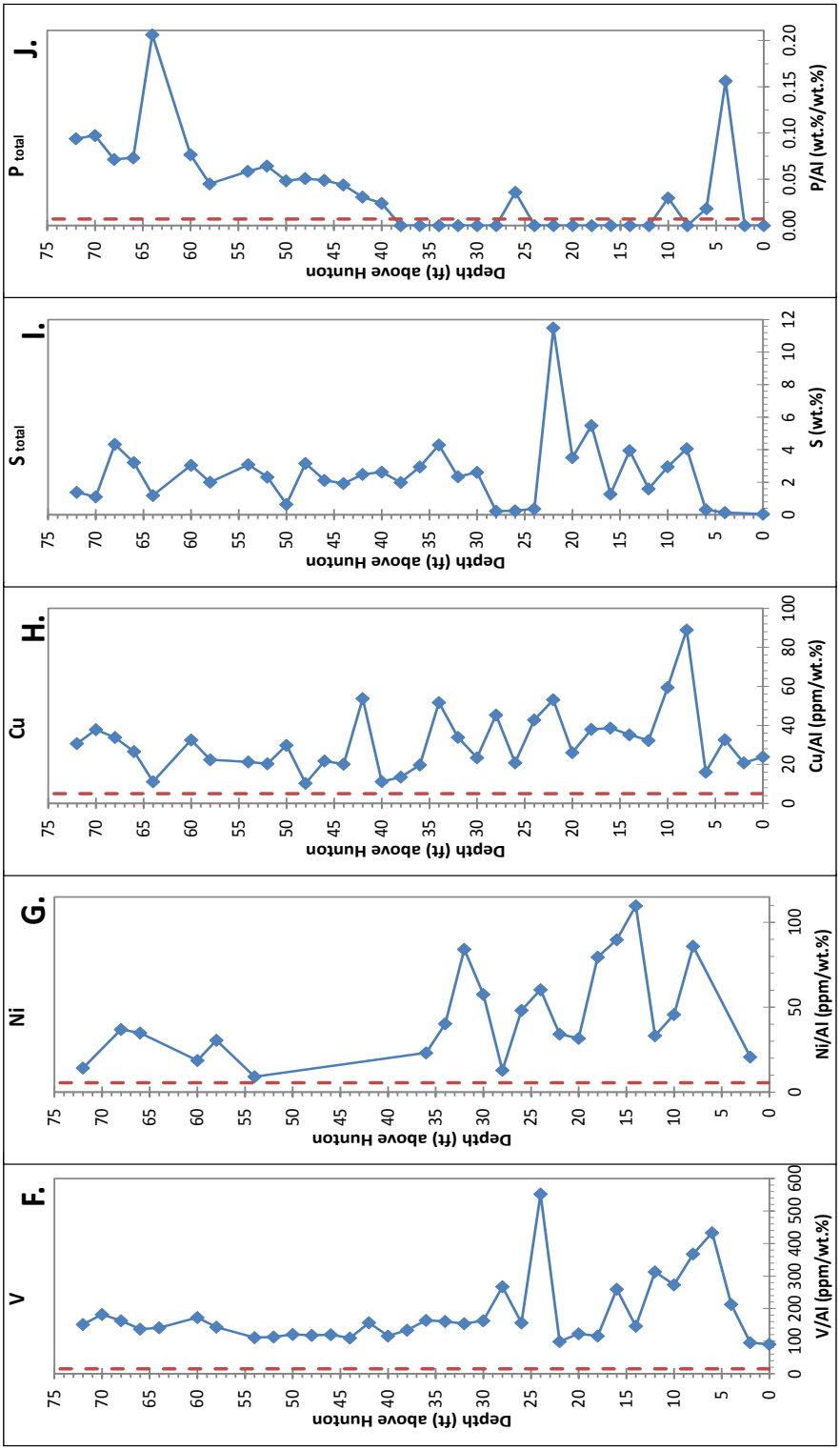

Figure 17 continued. (F) V/Al; (G) Ni/Al; (H) Cu/Al; (I) S/Al; and (J) P/Al.

.

CHAPTER V

DISCUSSION

Black shales in outcrop and hand sample may appear very similar, which could be interpreted as evidence that they were deposited under similar conditions. However, despite very similar visual appearances, these rocks can be deposited under a wide range of environmental conditions, such as differences in water depth, strength of surface or bottom currents, intensity of water-column productivity, types of organic matter, sedimentation rates, sediment accommodation, oxygen concentrations in the water column, and a host of other conditions. The principal controls on the accumulation of organic carbon in marine sediments include bulk sediment accumulation rate, water column anoxia, and the rate of supply of organic matter to the sea floor (Demaison and Moore, 1980). In more recent work on the efforts to resolve the debate on the dominate controls on organic matter accumulation, Bohacs et al., (2005) concluded that organic matter rich rocks are the result of complex, contingent interactions of competing rates of organic production, destruction, and dilution. The Woodford Shale is a highly organic-rich marine source rock, with much of the organic matter that rained onto the seafloor during Woodford deposition, chiefly within zooplankton fecal pellets, being preserved within the sediments, (Kirkland et al., 1992). At the McAlister Shale Pit

Kirkland et al. (1992), petrographically observed many species of microflora in the fossil assemblages, including spores and hystrichosphararids and planktons include *Foerstia sp*. (probably of algal affinity), *Tasmanites sp*. (an alga), and radiolaria. Kirkland et al. (1992) also considered one of the most important factors that contributed to the preservation of organic matter in the Woodford was the establishment of anoxic bottom water conditions that inhibited the respiratory activity of aerobic microorganisms. Under these conditions the algal organic matter is resistant to bacterial degradation and is well-preserved in sediments. Preservation of relatively high concentrations of organic carbon and an abundance of pyrite in the Woodford Shale are interpreted as evidence that the bottom waters were anoxic for prolonged periods of time (Comer, 2005).

While the outcrops at the McAlister Shale Pit and at Highway 77D are very similar in their overall lithologic characteristics, previous studies have shown that differences exist in the spectral gamma-ray signatures of the Woodford, both in a single section; as well as, between different locations (Watson, 2008; Krystiniak, 2005). Paxton et al. (2006), studied spectral gamma ray response from several outcrops of the Woodford Formation in south central Oklahoma and determined that the U content dominated the gamma ray response not K and Th. Comer's (1992) TOC calculations from a well in the same section as the McAlister Shale Pit were shown to be 10.3±5.4 wt%. Comer's (1992) TOC calculations from a well approximately 6 miles from the Highway 77D outcrop were shown to be 8.5 wt%. Such differences in TOC and U concentrations are likely related to differences in the paleoenvironmental conditions during deposition—especially changes in the presence and strength of bottom-water anoxia. Redox-sensitive trace element ratios are among the most widely used indicators of redox conditions in

modern and ancient sedimentary systems and exhibit considerable enrichment in laminated, organic rich facies, especially those deposited under anoxic and euxinic conditions (Algeo and Maynard, 2004; Calvert and Pedersen, 1993; Crusius et al., 1996). Observing and mapping these differences are very important to constrain paleoenvironmental conditions during deposition, and may potentially be applied to the search for petroleum deposits, both for assessing source rock characteristics as well as reservoir characterization in resource plays.

CORRELATION

Lithology

At both study areas the Woodford Shale unconformably overlies the Hunton Group (Kirkland et al., 1992; Neman, 2011). Previous workers have long assumed that the Woodford had low sedimentation rates because of the high organic carbon concentrations. Kirkland et al. (1992) calculated sedimentation rates by taking the thickness of the Woodford Formation at the McAlister Shale Pit and estimated that a duration of ~ 15 million years for deposition amounted to an average of approximately 0.01 mm sedimentation per year. In the modern ocean, concentrations of nutrients and organisms are not evenly distributed in surface waters or the water column. Thus organic productivity is not evenly distributed. It is expected that even with an overall slow sedimentation and high organic productivity, that there will be regional variations within deposition of the Woodford Shale. These regional variations not only occur at the same time in different locations, but can also occur at different times in the same location. This

is illustrated by the differences in lithologies up section at a single outcrop and when different localities are compared in detail.

The predominant lithology for the Woodford Shale is black shale but also includes chert, siltstone, sandstone, dolostone, and light colored shale (Comer, 2005; Amsden, 1975). Figure 18 shows the spectral gamma ray as well as lithologic differences in the outcrops at the McAlister Shale Pit and at Highway 77D. The outcrop at the McAlister Shale Pit consists of mostly black siliceous shale that varied in fissility and brittleness. The siliceous and fissile beds are irregularly spaced and vary in thickness, 2 to 6 inches, increase in frequency up section. The Woodford Shale at Highway 77D is also characterized by alternating fissile and silica rich beds. The chert beds here too are irregularly spaced and vary in thickness between 3 and 10 inches increase in frequency up section. The lithologies are broadly similar at both outcrops; however, the thickness of the informal members is different at the two study areas (Figure 18).

Geochemical Trends

The mechanisms for the development of anoxia remain highly debated, and typically center around two end members of high productivity or the presence of a restricted or silled basin that prevents renewal of bottom-water oxygen concentrations. It is generally accepted that black shales form in environments where the aqueous oxygen concentrations are low to zero at/or above the sediment water interface (Pederson and Calvert, 1990). Redox conditions strongly influence trace metal enrichment/depletion patterns, which are controlled by (1) solubilities of reduced versus oxidized species as either oxide or sulfide minerals, for example (Mn, Fe, V, Zn, Pb); (2) absorption of

reduced or oxidized species onto other authigenic minerals like Fe-oxyhydroxides (V, Zn, Ni); (3) preferential absorption of reduced species with organic carbon (U, Mo, Ni, U; Cruse and Lyons, 2004). U and V enrichment without Mo enrichment implies suboxic/anoxic deposition without the presence of aqueous H_2S (Tribovillard et al., 2006). Conversely, sediments exhibiting concurrent enrichments in U, V, and Mo likely reflect euxinic conditions at the sediment water interface or in the water column (Algeo and Maynard, 2004). Some of these redox-sensitive elements (Ni, Cu, Zn, Cd) are delivered to the sediment mainly in association with organic matter and they may be retained within the sediment in association with pyrite (Tribovillard et al., 2006).

Using the Pre-Woodford unconformity as the datum, TOC and metal/Al ratio concentrations are plotted versus depth above the Hunton Formation in Figures 16 and 17. These patterns of enrichment/depletion are used to correlate the outcrops of the McAlister Shale Pit and Highway 77D. Within both outcrops, the Al normalized concentration of the transition metals (Fe, Mo, U, V, Ni, Cu) are enriched relative to the PAAS standard. This suggests that there was low/zero oxygen present at/or above the sediment water interface throughout deposition of the Woodford Shale. Romero and Philp (2011) have conducted organic geochemical analysis on the Woodford Shale in an outcrop in Pontotoc County. From their analyses, they determined that high salinity conditions and water density stratification leading to suboxic/anoxic conditions prevailed during deposition of the entire Woodford Shale. Moreover, the chemocline (boundary between anoxic and oxic conditions in the water column) was located at shallower depths during Middle Woodford deposition as compared to times of deposition of the lower and upper members. Romero and Philp (2011) also concluded that presence of a water-

column chemocline varied during deposition of the lower and upper members (i.e., its presence was variable, likely reflecting more vigorous water-column circulation). This depositional model developed from organic geochemical data agrees with the patterns observed in metal/Al ratios for the middle and lower sections at the 77D outcrop and by the low metal/Al ratios in the middle section of the Woodford.

Due to the lack of measurements at the Hunton/Woodford unconformity at the McAlister Shale Pit, the use of spectral gamma ray logs is used to constrain the deposition of the Woodford shale between the two study areas. Approximately 50 ft. above the Hunton, where the transition-metal/Al ratios (Fe, Mo, U, V, Cu) show a marked increase compared to values in underlying samples (Figure 16). This increase is interpreted to reflect onset of fully anoxic/euxinic conditions in the water column. This coincides with an increase in the spectral gamma ray values, (Figures 17 and 16). This is consistent with the conclusions of Romero and Philp (2011), in which the Middle Woodford was deposited under anoxic conditions.

As deposition of the middle member continued there is a decrease in (Fe, Mo, U, V, Cu)/Al ratios up to ~100 ft. above the Hunton at McAlister Shale Pit. At the 77D outcrop, there is a spike in the (Fe, Mo, U, V, Ni, Cu)/Al ratios; however the ratios are half as enriched as those at the McAlister Shale Pit. Enrichments of metal/Al ratios and TOC from each outcrop do not appear to directly correspond to thickness and depth (Figure 16 and 17). This is again, further evidence that black shale deposition does not occur uniformly under the exact same conditions at a given time at all locations within a basin. This also implies that anoxic conditions did not start and stop at each outcrop at the same time, most likely due to uneven distributions of microorganisms and nutrients

(i.e., upwelling) in the surface waters, as well as the presence and depth of the chemocline in the water column. By examining differences in the chemostratigraphy of each outcrop, the paleoceanographic conditions during deposition can be better constrained.

PALEOCEANOGRAPHIC CONDITIONS

Bottom-Water Redox

Trace metal enrichments indicate redox conditions prevailing at the time of deposition and early diagenesis, which can allow us to reconstruct paleodepositional conditions (Algeo and Maynard, 2004; Rimmer, 2004). Anoxic/euxinic conditions are pervasive during the Woodford deposition at the McAlister Shale Pit, as indicated by the enrichment of U, V, and Mo relative to the PAAS standard (Tribovillard et al., 2006). There appears to be a shift in trace metal behavior above ~100 ft. at this location. The Mo/Al ratio shows less stratigraphic variation above 110 ft. Fe/Al ratio decreases through the same interval (Figure 16). There also appears to be marked increase in metal/Al ratios of Fe, Mo, U, V, and Cu at approximately 50 ft., this is interpreted to be the full onset of anoxic/euxinic conditions at McAlister Shale Pit.

Trace metal concentrations at 77D show higher frequency changes below 26 ft (Figure 17). Although the trace metals at the 77D outcrop are enriched relative to PAAS, the enrichment is half of that observed at McAlister Shale Pit. The average metal/Al ratios for Mo, U, and V are high at the McAlister Shale Pit (Mo=95.6, U=203.6, V=458.9) as compared to those at the 77D outcrop (Mo=43.3, U=93.8, V=180.9). These lower ratios likely indicate that there were times when more dissolved oxygen was

present in the water column at 77D than at the McAlister Shale Pit. This implies more dynamic water-column conditions at the 77D outcrop, as compared to the McAlister Shale Pit. This most likely is due to a shallower water-column at 77D, which is more easily affected by currents and overturning.

Algeo and Maynard (2004) have shown that black shales with >10% TOC and large enrichment factors of trace elements generally exhibit a weak covariation between TOC and trace metal concentrations. This is thought to be characteristic of trace elements of "strong euxinic affinity" or involved in other reactions catalyzed by free H_2S and resident mainly in authigenic phases such that enrichment in these trace metals (Mo, U, V) is not directly controlled by TOC concentrations. Trace metals versus TOC at the McAlister Shale Pit are poorly correlated (Figure 19), due to a high average of TOC value of 12.9%. This is consistent with euxinic conditions, such that trace metal enrichment is decoupled for TOC, because sufficient sulfide was present. However, at 77D, there is a better correlation between the metals and TOC (Figure 20). TOC concentrations at 77D are lower than the McAlister Shale Pit, 9.5%, this infers less-reducing conditions at 77D.

Productivity

Primary production of organic matter in the open ocean is accomplished by a wide range of unicellular planktonic organisms whose activities are governed by nutrient supply and solar radiation (Pedersen and Calvert, 1990). Biological factors influencing organic matter accumulation in sediments include primary biologic productivity of the surface water layers and biochemical degradation of dead organic matter by microbial

scavengers (Demaison and Moore, 1980). Anoxic conditions occur where the replenishment rate of dissolved oxygen to the water column is lower than its rate of consumption by aerobes (Pederson and Calvert, 1990).

Ni and Cu are dominantly delivered to the sediments in association with organic matter and are released through organic matter decay, thus if Ni and Cu are not scavenged by settling organic particles, they are not observed to be significantly enriched in the sediments (Tribovillard et al., 2006). High concentrations of Ni and Cu in sediments indicates (1) a high organic matter flux supplied these elements to the seafloor in abundance and (2) that reducing conditions were present, allowing Ni and Cu fixation within the sediments. This mechanism makes Ni and Cu good proxies for productivity (Tribovillard et al., 2006). At the McAlister Shale Pit Ni/Al and Cu/Al ratios are enriched relative to PAAS, with an average 71.6 and 55.1, for Ni and Cu, respectively. At Highway 77D Ni/Al and Cu/Al ratios were also enriched relative to PAAS, but to a lesser degree compared to the McAlister Shale Pit outcrop (Figures 16 and 17). The differences in the enrichments of the Ni/Al and Cu/Al ratios likely reflect differences in productivity at each outcrop, with a greater level of primary productivity at McAlister Shale Pit as compared to 77D. These differences likely reflect differences in their position relative to the locus of upwelling that would have driven primary productivity. The lower enrichments of the 77D outcrop are interpreted to be a result of an unstable chemocline due to a shallower water column.

Quartz (SiO_2) in mudstones can be both detrital and authigenic in origin. This difference in source has significant implications for a variety of areas, including basin modeling, palaeoclimate, palaeoproductivity, and biogeochemical silica cycling (Schieber

et al., 2000). The abundance of biogenic chert and marine organic matter indicates that there was high biologic productivity in the near surface waters of the epeiric sea during Woodford deposition (Comer, 2005). Kirkland et al. (1992) determined that the Woodford Shale in the Criner Hills area in Carter County is composed of approximately one-fifth organic matter, one-quarter illite, and the remainder silica by volume. The silica is derived largely from radiolaria and sponge spicules (Comer, 2005; Kirkland et al., 1992; Over, 1992). Cherts were most likely deposited during relatively short periods of siliceous productivity as organic-carbon-rich siliceous oozes, in contrast to shale deposition occurring over longer periods of time during lower levels of siliceous productivity (Roberts and Mitterer, 1992).

The relative contribution of silica from detrital or biogenic sources can be examined by normalizing Si concentrations to Zr. The only significant source of Zr to pelagic sediments is from terrigenous material, thus normalizing Si to Zr removes the effect of variable terrigenous input to these sediments (Snow et al., 2005). The Si/Zr ratio of PAAS is 0.31. When the calculated ratio exceeds this value, this likely indicates that Si is derived from an authigenic source (i.e., high levels of water-column productivity). The Si/Zr ratios at the McAlister Shale Pit show five pulses of enrichment relative to the PAAS standard. These pulses coincide with enrichments of P_{total} relative to PAAS (Figure 21A). Phosphorus plays a fundamental role in many metabolic processes and is released as PO_4^{3-} from decaying organic matter during oxic, suboxic and anoxic bacterial degradation below the sediment water interface (Tribovillard, 2006). Marine biological productivity is strongly controlled by the availability of the nutrient elements like P and N. It is believed that over geologic time, the ultimate limiting

nutrient has been P, thus a significant decrease in the abundance of dissolved P in the ocean should result in a corresponding decrease in marine productivity (Ingall et al., 1993). Figure 21A, demonstrates a possible correlation between Si/Zr ratio and P values, these coincident pulses of Si/Zr ratios with P_{total} enrichments may reflect high productivity.

The Si/Zr ratios at Highway 77D also show some enrichment relative to the PAAS standard in four zones (Figure 21B). Unlike McAlister Shale Pit, only two of these pulses coincide with enrichments in P_{total}, while the other two (11-24 ft and 28-38 ft) instead correspond to times when P was apparently not preserved in the sediments (Figure 21B). Easily metabolizable P is released from organic matter relative to organic carbon and the sediments can become depleted in metabolizable P, but may still contain metabolizable organic carbon which can be respired during further oxic diagenesis (Ingall et al., 1993). Two influential mechanisms for the storage and release of P are bacteria and redox cycling of Fe (Ingall, 1993; Tribovallard et al., 2006). Under oxic conditions bacteria can accumulate and store P and under anoxic conditions the stored P is utilized as an energy source and is released by bacteria to the surrounding solution (Ingall, 1993). Fe-oxyhydroxides that scavenge P from the sediment pore water are precipitated above the oxic/anoxic interface and dissolved below it (Tribovillard et al., 2006). Thus, times when Si/Zr does not correspond to enrichments in P result from times when dissolved oxygen was present indicating deposition under a less reducing water masses . Thus, these results are consistent with a model in which the water column at 77D is more oxidizing as compared to McAlister Shale Pit, which likely reflects an overall shallower water column at 77D relative to McAlister Shale Pit.

Deepwater Renewal Times

Changes in sedimentary Mo/TOC ratios are caused by both redox and the availability of Mo in bottom waters. Mo is not scavenged by TOC unless H_2S is present in the water column, dissolved sulfide converts MoO_4^{2-} to thiomolybdates at a critical H_2S (aq) threshold (the geochemical switch), transforming a geochemically inert form of dissolved Mo into a form that is readily scavenged by particles (Helz et al, 1996). As Mo is scavenged from the bottom waters, Mo concentrations can be depleted, resulting in a decrease in the Mo/TOC ratio—even if the flux of TOC to the sediments and euxinic/anoxic conditions remain unchanged. Mo/TOC ratios have been shown to be related to the renewal time of bottom waters in modern basins (Algeo and Lyons, 2006). Rowe et al. (2008) further showed how this model could be applied to ancient sediments (Barnett Shale) to establish hydrographic conditions during deposition. Mo/TOC ratios were calculated for the McAlister Shale Pit and Highway 77D samples (Figure 22) and plotted against estimated deep water renewal estimation times (Algeo and Lyons, 2006; Rowe et al., 2008; Figure 23). Deep water residence times varied throughout deposition of the Woodford Shale. The shortest estimated deep-water renewal times occur at 77D (~20 years), while at the McAlister Shale Pit, the shortest estimated deep-water renewal time was 300 years. Also, the overall range in estimated renewal times is much greater for 77D as compared to the McAlister Shale Pit. The changes in magnitude of the renewal times are interpreted to reflect the differences of the water column depths at both locations. The lower minimum times, and wider range in times, estimated for 77D reflect the relative shallower water column and ease of overturning—both seasonally and on

longer time scales. Rapid overturning renews Mo concentrations, leading to higher Mo/TOC ratios. Deep water renewal times estimated for McAlister Shale Pit tend to be of a longer duration compared to 77D, likely because of a deeper water column that stabilized anoxic/euxinic conditions because of the greater energy requirement to overturn a deeper water column. These differences are again consistent with variable water column conditions throughout the Devonian Sea, reflecting seafloor geometry and oceanographic conditions.

Depositional Model

The geochemical analysis of the McAlister Shale Pit and the 77D outcrop was used to generate a depositional model for the Woodford Shale in the Arkoma Basin (Figure 24, redrawn from Watson (2008)). Watson (2008) studied outcrops and core from south central Oklahoma and south east Missouri and developed an inferred depositional model. In this context, the geochemical data collected was used for the placement of the study areas in their relative locations on the paleoshelf.

In this refined model, the 77D outcrop is located more proximal to the shoreline, in shallower waters, than the McAlister Shale Pit. Higher metal/Al ratios at the McAlister Shale Pit as compared to 77D indicate that the water column at the McAlister Shale Pit was generally more reducing, on average, than at 77D. Higher metal/Al ratios together with higher TOC concentrations are interpreted to indicate that the McAlister Shale Pit was located in generally deeper waters relative to 77D.

Higher TOC concentrations at the McAlister Shale Pit relative to 77D can be attributed to a greater preservation potential due to a more reducing water column.

However, Ni/Al and Cu/Al ratios are thought to be indicators of water-column productivity (Tribovillard et al., 2006). The Ni/Al and Cu/Al ratios are higher at the McAlister Shale Pit than at 77D, indicating that the more reducing water column at the McAlister Shale Pit resulted from a greater flux of TOC to the sediments from high rates of productivity in the overlying water column. Primary productivity is limited by the availability of nutrients in the surface waters. The main mechanism to deliver nutrients to surface waters is upwelling of deep (nutrient-rich) waters. Thus, the higher productivity at the McAlister Shale Pit as compared to 77D can constrain the geographic location of the most intense upwelling (Figure 24).

The TOC concentrations and the Ni/Al ratios are consistent with the higher Si/Zr ratios; while their relationship with P indicates more preserved pulses of radiolarian productivity at the McAlister Shale Pit than at 77D, supporting the conclusion that the McAlister Shale Pit was closer to the upwelling location. The enrichments in P come from the productivity and the anoxic bottom waters at the McAlister Shale Pit. There was at least one occurrence of upwelling/productivity at the McAlister Shale Pit that was not observed at the 77D outcrop. Furthermore, occurrences at 77D, where no P is preserved in the sediments, are consistent with less reducing/ weaker stratification of the water column.

The Mo/TOC ratios at the McAlister Shale Pit show longer estimated deep water renewal times. The lower minimum deep water renewal times and the wider range of time that is estimated for 77D, reflect the relatively shallower water column and its ease of overturning—both seasonally and on longer time scales.

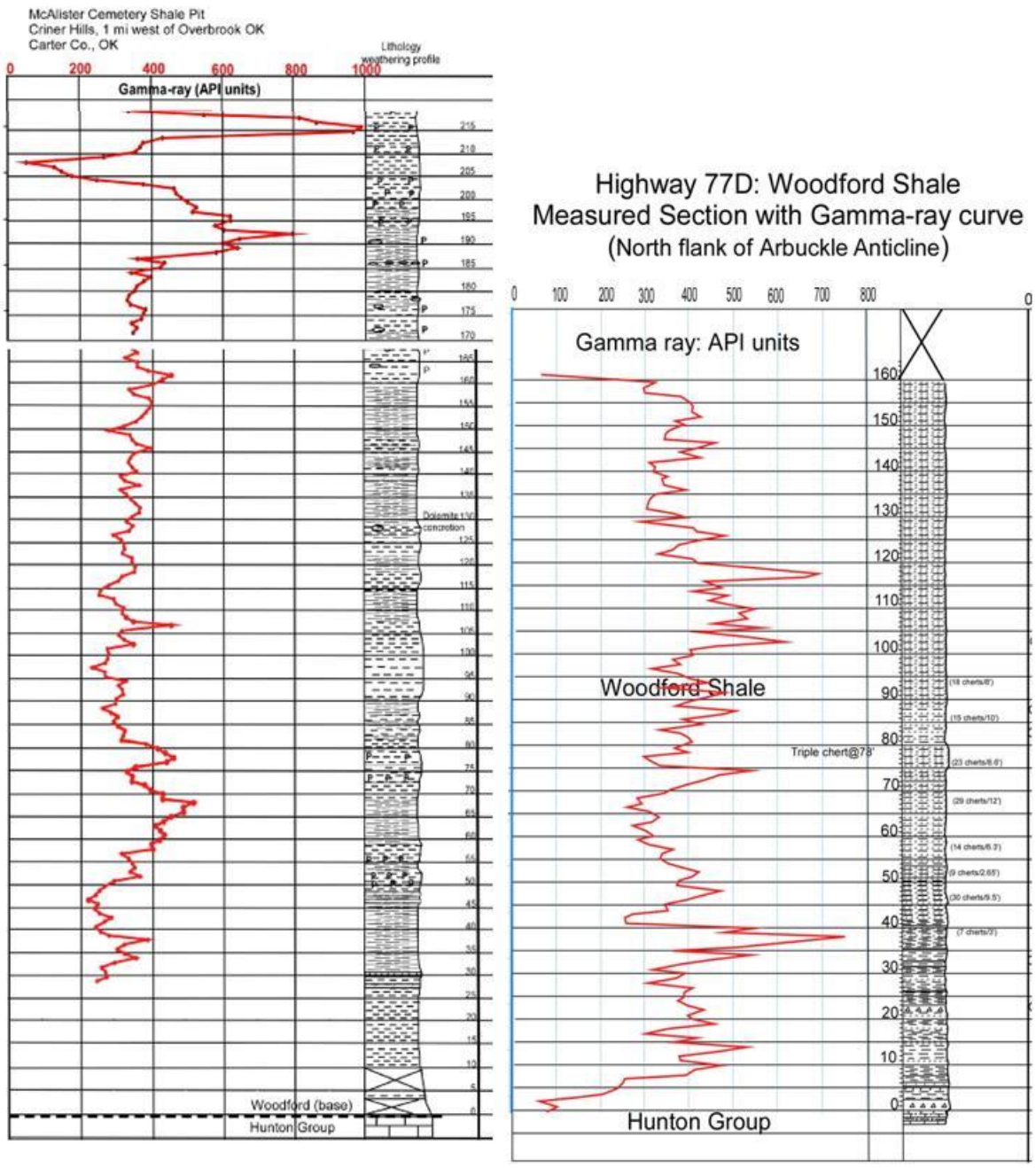

Figure 18. Spectral gamma ray and lithological profiles for the McAlister Shale Pit and Highway 77D. Datum is the Pre-Woodford Unconformity. Scale in feet above Hunton Formation. (From Puckette et al., 2010, personal communication).

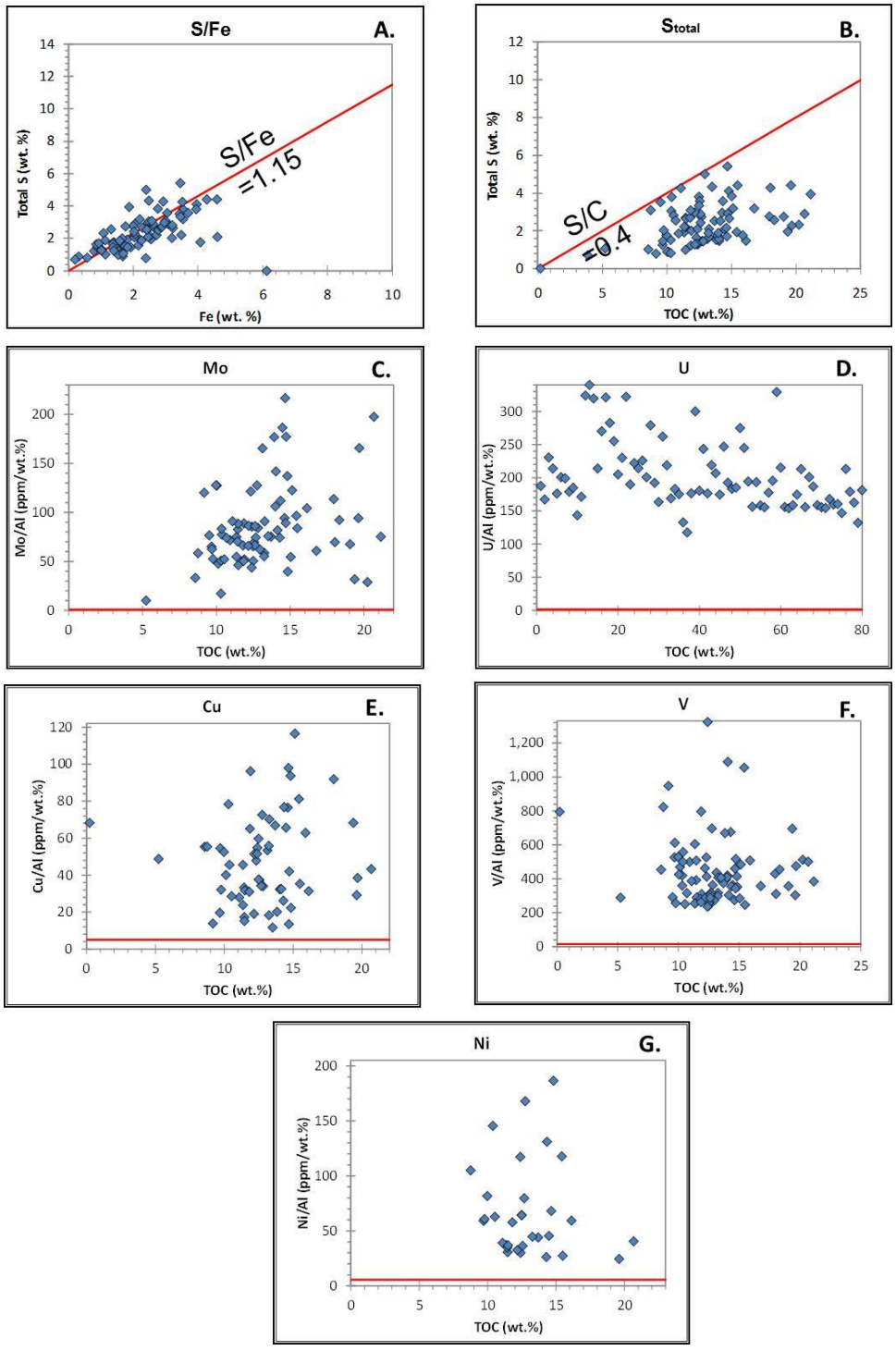

Figure 19. Cross-plots from the McAlister Shale Pit showing relationships between C, total S, total Fe and key trace elements: **(A)** total S vs. total Fe; **(B)** total S vs. TOC; **(C)** Mo vs. TOC; **(D)** U vs. TOC; **(E)** Cu vs. TOC; **(F)** V vs. TOC; and **(G)** Ni vs. TOC. S/Fe line in Fig. 19 A is the line for stoichiometric pyrite. S/C line in Fig. 19 B is the Holocene normal marine line (Raiswell and Berner, 1983). Red lines in Figs. 19 C-G represent the concentration ratio in the Post-Archean Average Shale (PAAS; Taylor and McClennan, 1985).

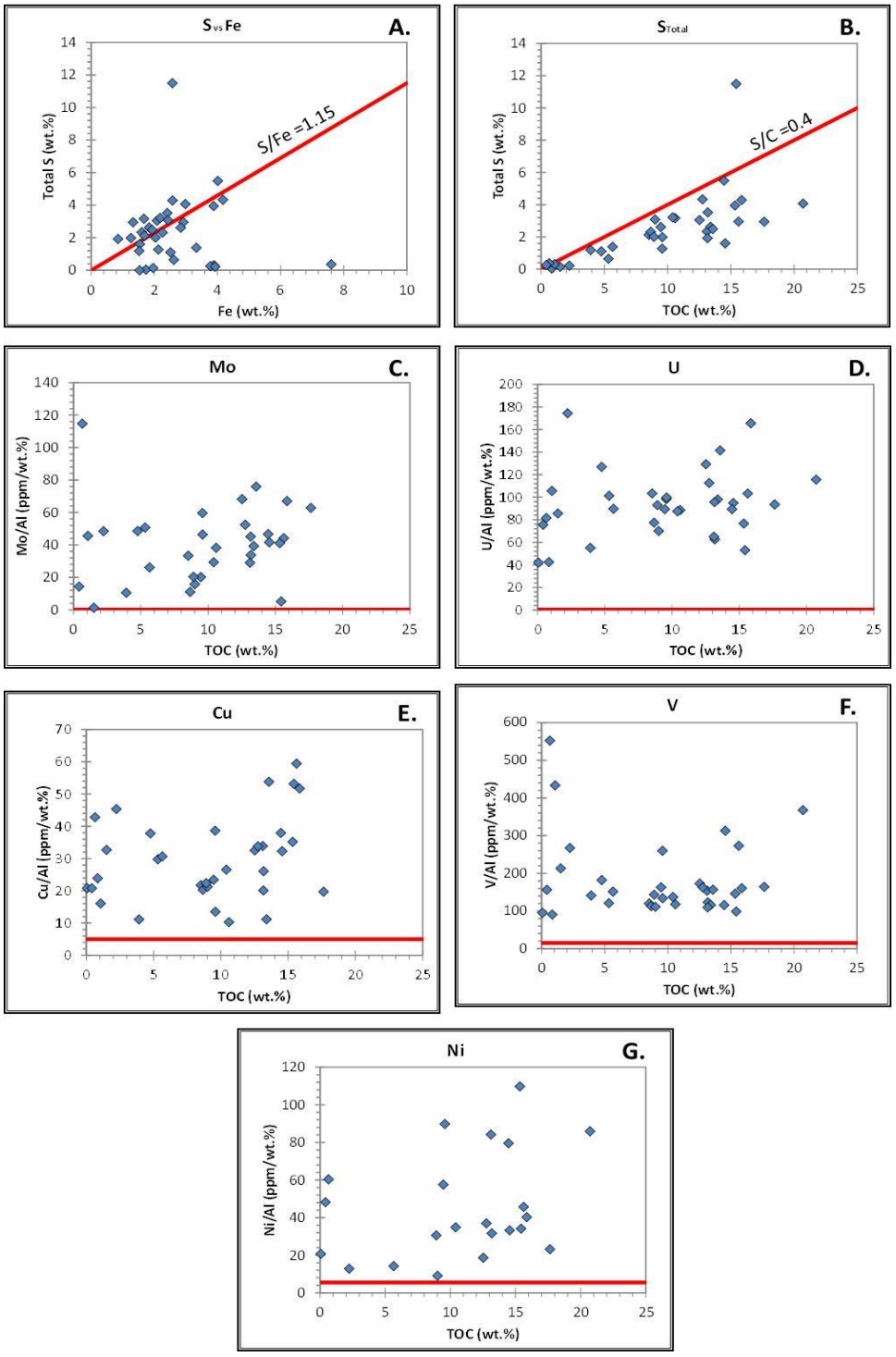

Figure 20. Cross-plots from the Highway 77D outcrop showing relationships between C, total S, total Fe and key trace elements: **(A)** total S vs. total Fe; **(B)** total S vs. TOC; **(C)** Mo vs. TOC; **(D)** U vs. TOC; **(E)** Cu vs. TOC; **(F)** V vs. TOC; and **(G)** Ni vs. TOC. S/Fe line in Fig. 20 A is the line for stoichiometric pyrite. S/C line in Fig. 20 B is the Holocene normal marine line (Raiswell and Berner, 1983). Red lines in Figs. 20 C-G represent the concentration ratio in the Post-Archean Average Shale (PAAS; Taylor and McClennan, 1985).

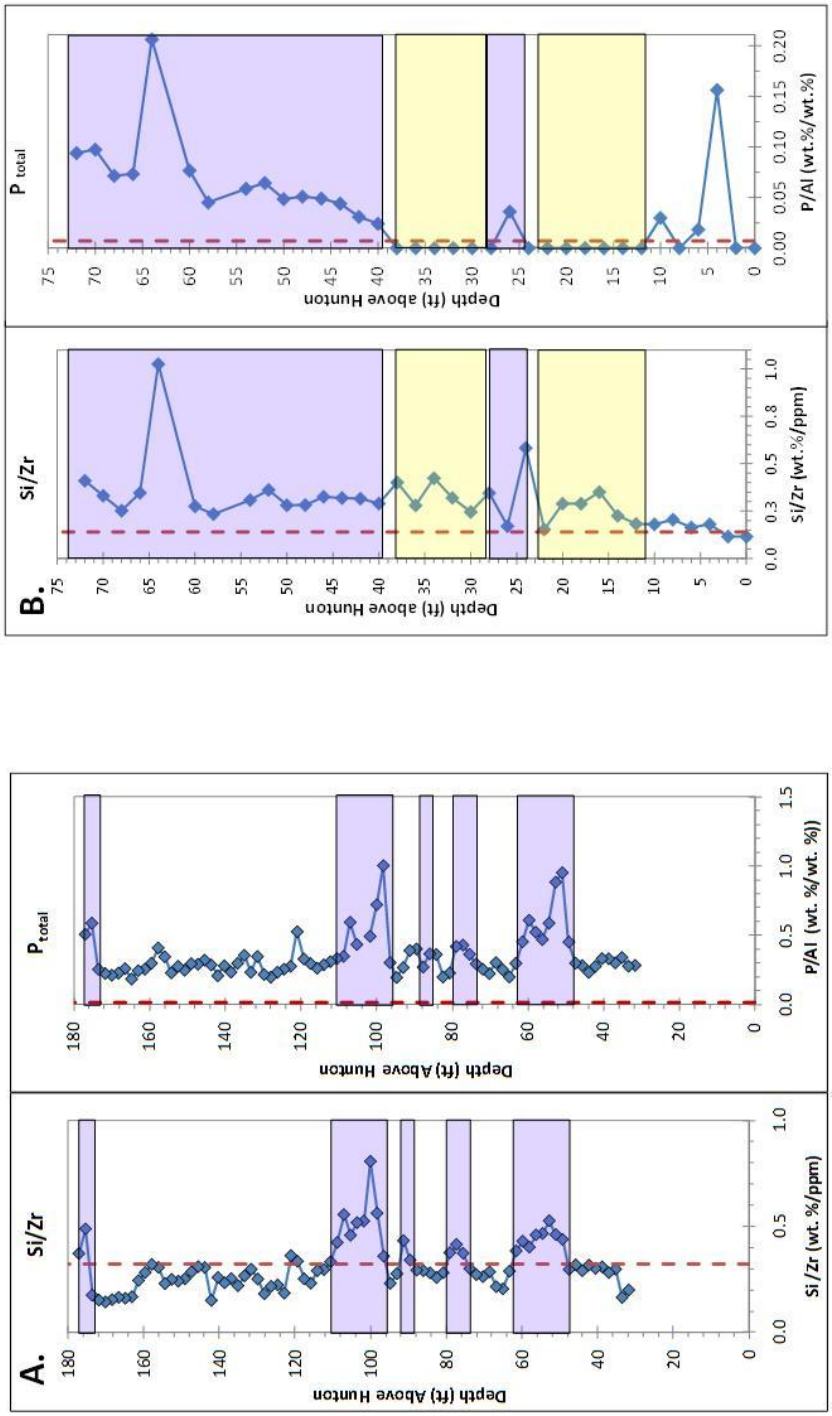

Figure 21. Si/Zr ratios and P_{total} are plotted versus depth above the Hunton, A) McAlister Shale Pit and B) 77D. Purple boxes indicate intervals where excess Si that coincides with elevated total P concentrations. Yellow boxes indicate intervals where Si is enriched, but P was not preserved. Dashed red lines represent the concentration ratio in the Post-Archean Average Shale (PAAS; Taylor and McClennan, 1985).

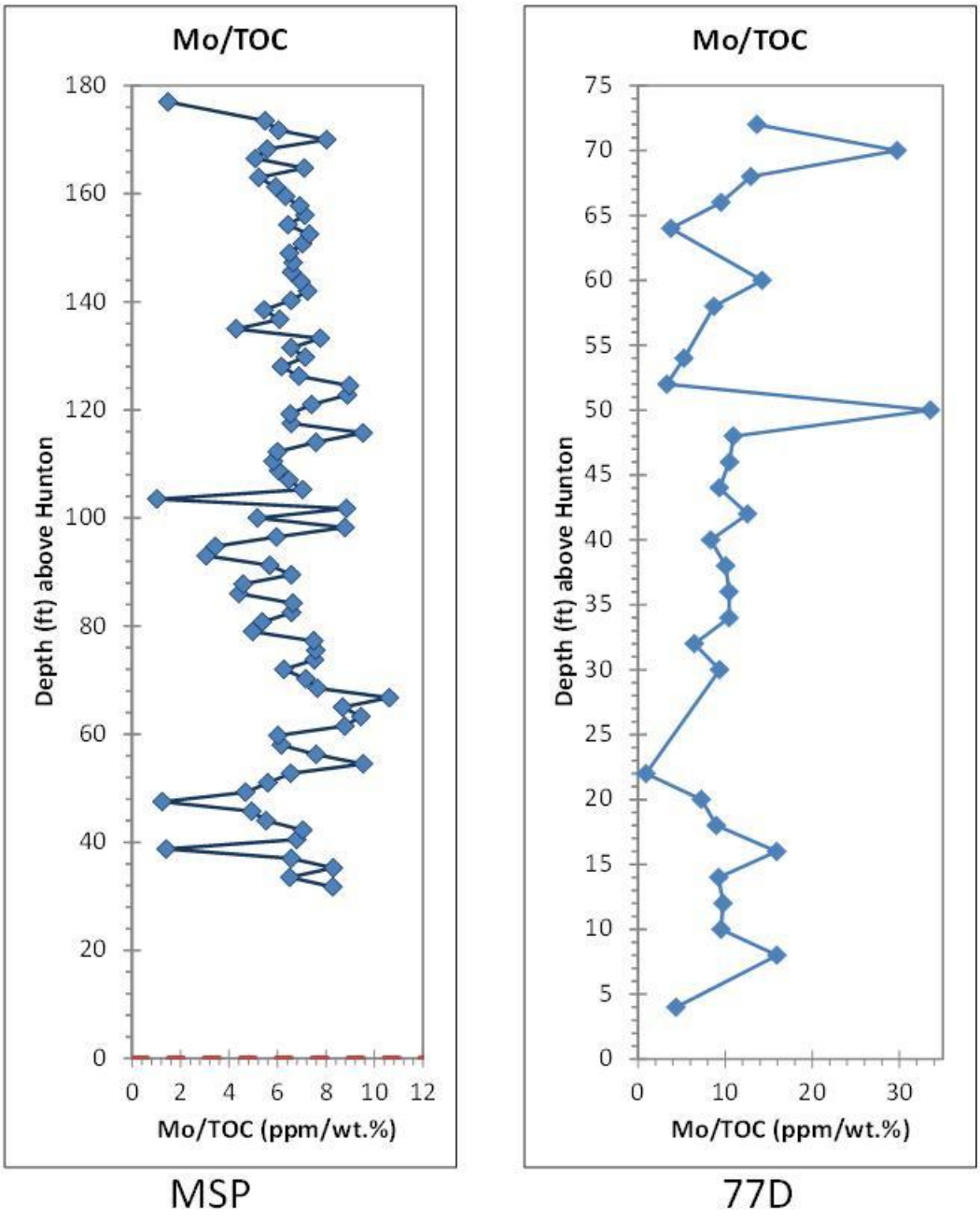

Figure 22. Mo/TOC ratios from the McAlister Shale Pit and Highway 77D versus depth above the Hunton Formation.

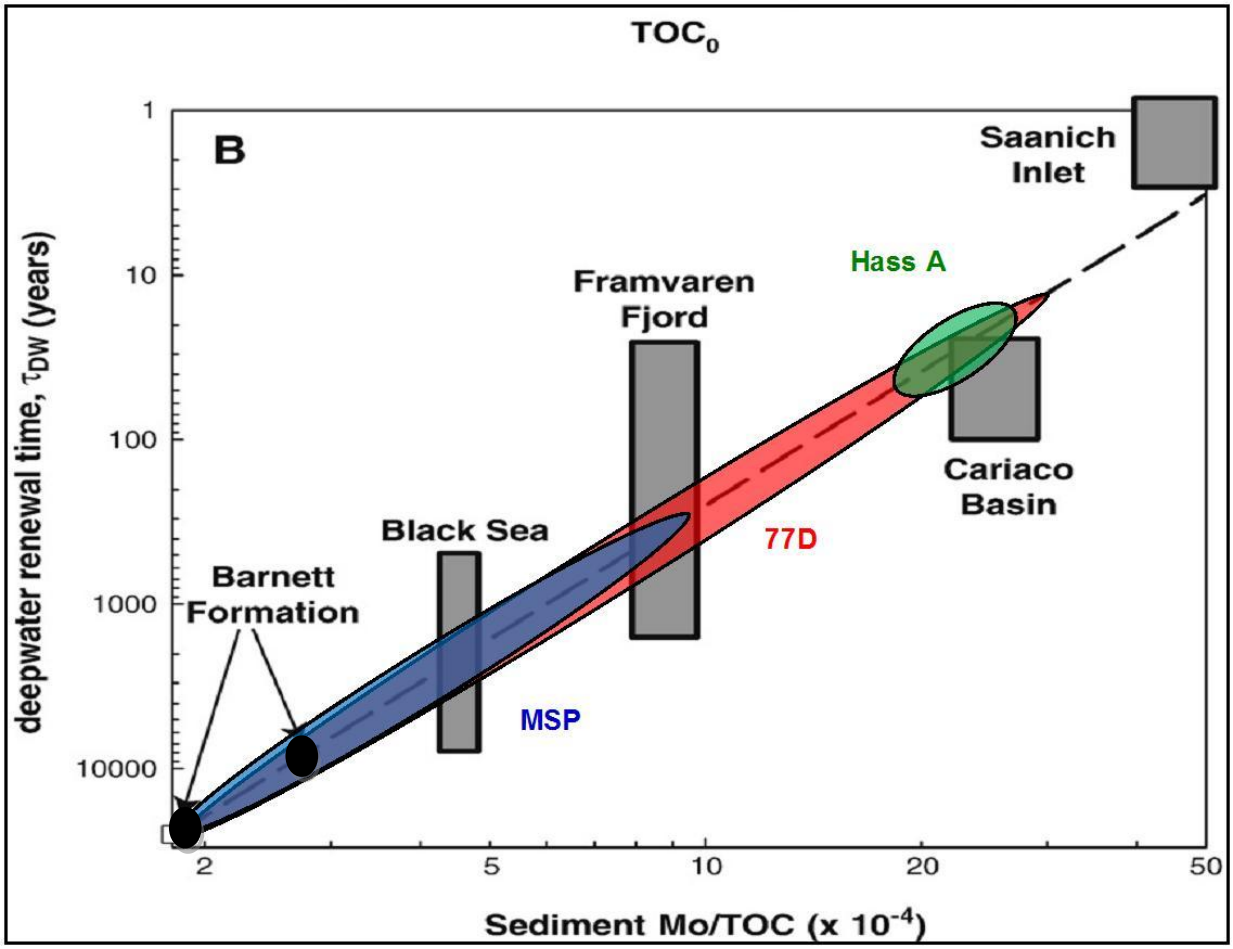

Figure 23. Inferred deep water renewal times for McAlister Shale Pit and Highway 77D based on Mo/TOC ratios. Black boxes are data from modern anoxic/euxinic basins from Algeo and Lyons (2006) work on modern anoxic basins. Black circles are the Barnett Shale (Rowe et al., 2008). Figure modified from Rowe et al. (2008).

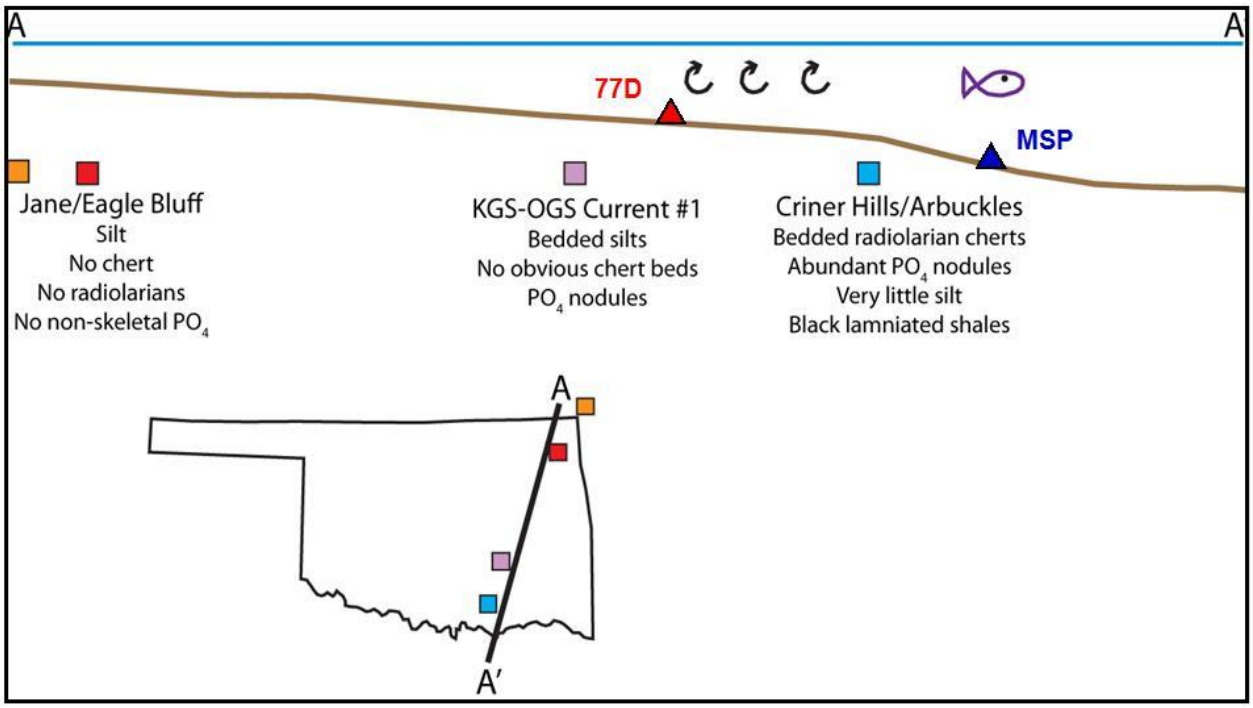

Figure 24. Inferred depositional model for Devonian dark shales in Oklahoma showing sites of McAlister Shale Pit and Highway 77D in this study and other key locations. Redrawn from Watson (2008).

CHAPTER VI

CONCLUSIONS

Observing and mapping the geochemical differences in marine black shales is very important for constraining paleoenvironmental conditions during deposition, and may potentially be applied to the search for petroleum deposits, both for assessing source rock characteristics, as well as reservoir characterization in resource plays. The Woodford Shale is a major unconventional play in the Mid-continent and understanding the paleoenvironmental conditions during deposition will help with basin analysis and exploration of the Woodford formation.

Based on the geochemical analysis of TOC concentrations and trace element ratios from Woodford Shale outcrops located at the McAlister Shale Pit in Carter County and at Highway 77D in Murray County in south-central Oklahoma, allowed for the placement of the two Woodford Shale outcrops onto an inferred depositional model. In this refined model, the 77D outcrop is located more proximal to the shoreline, in shallower waters, than the McAlister Shale Pit. Higher metal/Al ratios together with higher TOC concentrations are interpreted to indicate that the McAlister Shale Pit was located in generally deeper waters relative to 77D. Evidence for the placement of the study areas in the model is as follows: 1) the metal/Al ratios at 77D are half that of the

McAlister Shale Pit ratios, indicating there may have been more dissolved oxygen present in the water column, which infers more dynamic bottom waters; 2) the productivity indicators (Ni, Cu) are lower at the 77D outcrop and are interpreted to be the result of an unstable chemocline from a shallower water column; 3) the Si/Zr ratios do not always correspond to enrichment of P at 77D, unlike the ratios at the McAlister Shale Pit. Thus, times when the Si/Zr ratios do not correspond to enrichments in P result from times when dissolved oxygen was present indicating deposition under a less reducing water mass; 4) The Mo/TOC ratios at 77D exhibited a wider range, which reflects renewal of Mo concentrations. The lower minimum deep water renewal times that is estimated for 77D, reflect the relatively shallower water column and its ease of overturning.

Future Work

To further the understanding of the depositional environment and the bottom water redox conditions of the Woodford Shale, an expanded geochemical analysis including additional Woodford outcrops should be conducted and incorporate other geochemical techniques such as the degree of pyritization (DOP) analysis. Radiometric dating and a detailed biostratigraphic study would allow for the calculation of sedimentation rates and organic matter accumulation. The collection of these kinds of data could be combined to create detailed geochemical facies maps to understand the regional distribution of redox conditions of various depositional environments.

REFERENCES

Algeo, T. J. and Maynard, J. B., 2004, Trace element behavior and redox facies in core shales of Upper Pennsylvanian Kansas type cyclothems, Chemical Geology, v. 206, p. 289-318.

Algeo, T. J., and Lyons, T. W., 2006, Mo-total organic carbon covariation in modern anoxic marine environments: Implications for analysis of paleoredox and paleohydrographic conditions, Paleoceanography, v. 21, p. 1-23.

Allen, Robert W., 2000, Stratigraphy, Mountain Building and Complex Geological Structures of the Ardmore Basin, OCGS- The Shale Shaker, July-December, p. 10-21.

Amsden, T., and Klapper, G., 1972, Misener Sandstone (Middle-Upper Devonian), North-Central Oklahoma, AAPG Bulletin, v. 56, p. 2323-2334.

Amsden, T. W., 1975, Hunton Group (Late Ordovician, Silurian, and Early Devonian) in the Anadarko Basin of Oklahoma: Oklahoma Geological Survey Bulletin, p. 121-214.

Amsden, T. W., 1989, Depositional and post-depositional history of Middle Paleozoic (Late Ordovician through Early Devonian) strata in the ancestral Anadarko Basin, Oklahoma Geological Survey, v. 90, p.143-146.

Arthur, M. A., and Sageman, B. B., 1994, Marine black shales: depositional mechanisms and environments of ancient deposits, Annual Review of Earth and Planetary Sciences, v. 22, p. 499-551.

Betts, J. and Holland, H., 1991, The oxygen content of ocean bottom waters, the burial efficiency of organic carbon, and the regulation of atmospheric oxygen, Global and Planetary Change, v. 5, p. 5-18.

Bohaca, K. B., Grabowski Jr., G. J., Carroll, A. R., Mankiewicz, P. J., Miskell-Gerhardt, K. J., Schwalback, J. R., Wegner, M. B., and Simo, J. A., 2005, Production, dilution—the many paths to source-rock development, Society for Sedimentary Geology, Special Publication, v. 82, p. 61-101.

Boardman D, 2011, Preliminary analysis of phosphate nodules in the Woodford Shale, Late Devonian-Early Mississippian, southern Oklahoma, Oklahoma State University, Master's Thesis.

Calvert, S. and Pedersen, T., 1993, Geochemisty of recent oxic and anoxic marine sediments: implications for the geological record, Marine Geology, v. 113, p. 67-88.

Calvert, S., Bustin, R., and Ingall, E., 1996, Influence of water column anoxia and sediment supply on the burial and preservation of organic carbon in marine shales, Geochimica et Cosmochimica Acta v. 60, p. 1577-1593

Cardott, B., and Lambert, M., 1985, Thermal maturation by vitrinite reflectance of Woodford Shale, Anadarko Basin, Oklahoma, AAPG Bulletin, v. 69, p. 1982-1998.

Cardott, B., 2005, Overview of unconventional energy resources of Oklahoma, Circular-Oklahoma Geological Survey, p. 7-18.

Comer, J. B., 1984, Petrologic factors controlling the internal migration and explulsion of petroleum form source rocks: the Woodford-Chattanooga of Oklahoma and Arkansas, Oklahoma City Geological Society, p. 197.

Comer, J.,1992, Organic geochemistry and Paleogeography of Upper Devonian Formations in Oklahoma and Northwestern Arkansas, Oklahoma Geological Survey Circular, p. 70-93.

Comer, J. B., 2005, Facies distribution and hydrocarbon production potential of Woodford Shale in the Southern Midcontinent, Oklahoma Geological Survey, p. 51-62.

Cruse, A. and Lyons, T., 2004, Trace metal record of regional paleoenvironmental variability in Pennsylvanian (Upper Carboniferous) black shales, Chemical Geology, v. 206, p. 319-345.

Cruse, A, 2010, Schematic Figures, Personal Correspondence.

Crusius, J., Calvert, S., Pederson, T., and Sage, D., 1996, Rhenium and molybdenum enrichments in sediments as indicators of oxic, suboxic and sulfidic conditions of deposition, Earth and Planetary Science Letters, v. 145, p. 65-78.

Demaison, G. and Moore, G., 1980, Anoxic environments and oil source bed genesis, Organic Geochemistry, v. 2, p. 9-31.

Hass, W., and Huddle, J., 1965, Late Devonian and Early Mississippian age of the Woodford Shale in Oklahoma, as determined form conodonts, U. S. Geological Survey Professional Paper, .D125-D132.

Helz, G. R., Miller, C. V., Charnock, J. M., Mosselmans, J. F. W., Pattrick, R. A. D., Garner, C. D., and Vaughn, D. J., 1996, Mechanisims of molybdenum removal from the sea and its concentration in black shales: EXAFS evidence, Geochim. Cosmochim. Acta 60, p. 3631-3642.

Henry, M., and Hester, T., Anadarko Basin Province (058),USGS

Hester, T. C., Schmoker, J.W., and Sahl, H.L., 1990, Log-derived regional source-rock characteristics of the Woodford Shale, Anadarko Basin, Oklahoma, Geological Survey Bulletin, p. D1-D38.

Ingall, E. D., Bustin, R. M., and Cappellen, P., 1993, Influence of water column anoxia on the burial and preservation of carbon and phosphorus in marine shales, Geochimica et Cosmochimica Acta, v. 57, p. 303-316.

Kirkland, D., Denison, R., Summers, D., and Gormly, J., 1992, Geology and organic geochemistry of the Woodford Shale in the Criner Hills and western Arbuckle Mountains, Oklahoma, Oklahoma Geological Survey, Circular 93, p. 38-69.

Krystyniak, A., 2003, Outcrop-based gamma ray characterization of the Woodford Shale of south-central Oklahoma, Master's Thesis, Oklahoma State University.

Lambert, M., 1993, Internal stratigraphy and organic facies of the Devonian-Mississippian Chattanooga (Woodford) Shale in Oklahoma and Kansas: chapter 11, AAPG Special Volumes, SG 37, p. 163-176.

Neman, R. L., 2011, My favorite outcrop-The Sylvan Shale, the Hunton Group, and the Woodford Shale, Oklahoma City Geological Society, v. 61, p. 343-349.

Over, J., 1992, Conodonts and the Devonian-Carboniferous boundary in the Upper Woodford shale, Arbuckle Mountains, South-Central Oklahoma, Journal of Paleontology, c. 66, p. 293-311.

Paxton, S., Cruse, A., and Krystyniak, A., 2006, Detailed fingerprints of global sea-level change revealed in Upper Devonian/Mississippian Woodford Shale of south-central Oklahoma, Search and Discovery, #40210.

Pedersen, T. and Calvert, S., 1990. Anoxia vs. productivity: What controls the formation of organic-carbon-rich sediments and sedimentary rock?, AAPG Bulletin, v. 74, p. 454-466.

Piper, D. and Calvert, S., 2009, A marine biogeochemical perspective on black shale deposition, Earth-Science Reviews, v. 95, p. 63-96.

Puckette, J., 2010, Gamma Ray Profile, Personal Correspondence.

Rimmer, S. M., 2004, Geochemical paleoredox indicators in Devonian-Mississippian black shales, Central Appalachian Basin (USA), Chemical Geology, v. 206, p. 373-391.

Roberts, C. T., and Mitterer, R. M., 1992, Laminated black shale-bedded chert cyclicity in the Woodford Formation, Southern Oklahoma, Oklahoma Geological Survey, p. 330-336.

Rowe, H., Loucks, R., Ruppel. S., and Rimmer, S., 2008, Mississippian Barnett Formation, Fort Worth Basin, Texas: Bulk geochemical inferences and Mo-TOC constraints on the severity of hydrographic restriction, Chemical Geology, v. 257, p. 16-25.

Schieber, J., Krinsley, D., and Riciputi, L., 2000, Diagenetic origin of quartz silt in mudstones and implications for silica cycling, Nature (London), v. 406, p 981-985.

Snow, J. L., Duncan, R. A., and Bralower, T. J., 2005, Trace element abundances in the Rock Canyon Anticline, Pueblo, Colorado, marine sedimentary section and their releationship to Caribbean Plateau construction an ocean anoxic event 2, Paleoceanography, v. 20 p. 1-14.

Taft, 1904, Preliminary report on the geology of the Arbuckle and Wichita Mountains in Indian Territory and Oklahoma, US Geologic Survey Professional Paper 31, p. 1-81.

Taylor and McLennan, 1985, The continental crust: Its composition and evolution, Blackwell Scientific Publications, Oxford.

Tribovellard, N., Algeo, T., Lyons, T., and Riboulleau, A., 2006, Trace metals as paleoredox and paleoproductivity: An update, Chemical Geology, v. 232, p. 12-32.

Tyson, R., 2001, Sedimentation rate, dilution, preservation and total organic carbon; some results of a modeling study, Organic Geochemistry, v. 32, p. 333-339.

Watson, B., 2008, Internal stratigraphy, composition and deposition setting of the Woodford Shale in southern Seminole County, Oklahoma, p. 141.

Wignall,P. and Maynard, J., 1993, The sequence stratigraphy of transgressive black shales, AAPG Special Volumes, v. SG 37: Source Rocks in a Sequence Stratigraphic Framework, p. 35-47.

.

APPPENDIX

Table 1.
Geochemical data from McAlester Shale Pit, Oklahoma

Sample	Depth (ft) above Hunton	TOC (wt%)	Al (wt%)	Fe (wt%)	Mo (ppm)	U (ppm)	Mn (ppm)	V (ppm)	Ni (ppm)	Cu (ppm)	S (wt%)	P (wt%)
MSP 01	31.75	12.41	1.20	1.51	102.6	225.3	65.8	1589.8	36.0	54.8	1.3	0.34
MSP 02	33.5	14.29	1.25	2.45	93.0	209.6	102.1	845.2	32.8	26.2	3.0	0.35
MSP 03	35.25	12.76	0.83	1.92	105.7	191.2	227.1	577.3	139.2	72.6	1.5	0.28
MSP 04	37	11.36	0.99	2.20	74.5	212.6	186.2	601.1	36.7	45.5	1.9	0.30
MSP 05	38.75	19.37	0.85	2.54	27.0	149.7	235.7	590.7	< LOD	68.2	2.0	0.28
MSP 06	40.5	16.14	1.05	1.53	109.4	210.7	77.7	1626.8	62.1	31.3	1.5	0.35
MSP 07	42.25	15.42	1.12	1.81	108.5	223.9	< LOD	1185.4	132.3	81.2	1.9	0.31
MSP 08	44	8.58	1.43	1.13	47.4	255.3	< LOD	647.2	< LOD	55.4	1.0	0.33
MSP 09	45.75	10.13	1.05	1.67	49.9	193.5	< LOD	490.5	< LOD	40.1	0.9	0.29
MSP 10	47.5	20.24	0.87	1.08	25.1	124.7	< LOD	445.8	< LOD	< LOD	2.3	0.26
MSP 11	49.25	11.87	0.63	0.78	55.5	107.1	59.6	497.7	< LOD	65.0	1.2	0.28
MSP 12	51	14.07	0.34	0.88	78.7	110.5	< LOD	371.4	< LOD	< LOD	1.5	0.32
MSP 13	52.75	13.83	0.34	1.42	90.4	115.7	< LOD	227.6	< LOD	20.1	1.5	0.30
MSP 14	54.5	15.90	0.50	1.40	151.5	160.7	< LOD	255.1	< LOD	62.9	1.8	0.29
MSP 15	56.25	13.92	0.60	1.38	105.6	127.8	< LOD	236.1	< LOD	< LOD	1.8	0.28
MSP 16	58	14.72	0.51	2.06	90.6	138.2	< LOD	264.3	< LOD	42.0	2.9	0.27
MSP 17	59.75	13.13	0.48	1.69	79.0	153.4	65.2	208.4	< LOD	53.4	1.6	0.29
MSP 18	61.5	14.48	0.68	2.03	126.9	192.4	< LOD	246.7	30.9	65.6	2.1	0.31
MSP 19	63.25	14.81	1.02	3.96	139.8	260.4	80.7	422.1	190.2	93.7	4.1	0.30
MSP 20	65	14.62	1.35	2.51	126.9	276.3	44.7	369.3	< LOD	76.5	2.2	0.27
MSP 21	66.75	20.67	1.11	3.08	219.1	255.3	60.5	555.3	44.8	43.3	2.9	0.28
MSP 22	68.5	15.13	0.94	3.54	115.6	304.1	104.2	456.5	194.0	116.5	3.2	0.29
MSP 23	70.25	13.70	1.30	2.42	98.1	247.5	42.7	489.3	57.4	66.9	2.5	0.29
MSP 24	72	10.31	1.27	1.74	64.5	281.7	< LOD	530.5	< LOD	78.3	1.5	0.32
MSP 25	73.75	13.27	1.10	2.45	99.7	235.1	< LOD	447.2	49.0	70.1	2.1	0.32
MSP 26	75.5	14.35	0.97	3.05	108.6	219.3	52.8	344.9	127.1	76.8	3.6	0.35
MSP 27	77.25	14.04	0.74	2.15	105.0	148.7	53.0	310.6	< LOD	32.3	1.6	0.32
MSP 28	79	17.95	0.79	1.99	89.2	219.1	< LOD	337.2	< LOD	91.9	2.8	0.33
MSP 29	80.75	11.90	1.23	1.65	63.9	236.0	< LOD	379.9	< LOD	96.2	2.0	0.28
MSP 30	82.5	13.25	1.49	1.36	87.0	242.8	< LOD	471.0	< LOD	18.3	1.7	0.29
MSP 31	84.25	19.68	0.79	2.04	130.5	206.4	< LOD	374.3	< LOD	38.4	2.3	0.28
MSP 32	86	18.33	0.87	1.31	80.7	191.1	< LOD	397.4	< LOD	< LOD	2.6	0.32
MSP 33	87.75	13.23	1.10	2.25	60.5	184.9	< LOD	327.3	< LOD	55.9	1.9	0.30
MSP 34	89.5	14.00	0.87	1.12	91.8	158.4	< LOD	353.6	< LOD	< LOD	1.9	0.35
MSP 35	91.25	11.46	0.79	1.53	65.0	137.6	< LOD	308.0	< LOD	17.3	1.0	0.31
MSP 36	93	14.84	1.14	2.28	45.4	151.9	< LOD	403.0	< LOD	22.3	2.7	0.30
MSP 37	94.75	5.24	1.78	1.68	17.9	208.5	59.7	512.4	< LOD	48.7	1.1	0.35
MSP 38	96.5	12.82	0.91	1.36	76.3	160.0	< LOD	328.3	< LOD	34.0	1.4	0.27
MSP 39	98.25	12.30	0.28	0.85	107.9	85.4	< LOD	149.7	< LOD	< LOD	1.6	0.28
MSP 40	100	10.04	0.41	0.31	51.9	73.5	< LOD	173.1	< LOD	< LOD	0.9	0.29
MSP 41	101.75	14.66	0.60	0.93	129.5	145.5	< LOD	275.1	40.7	97.9	1.7	0.29
MSP 42	103.5	3.90		0.19	4.0	89.0	< LOD	53.5	< LOD	< LOD	0.7	0.33
MSP 43	105.25	12.33	0.71	1.03	86.6	125.8	< LOD	294.4	< LOD	47.8	1.3	0.31
MSP 44	107	9.18	0.49	2.39	59.3	108.1	< LOD	467.7	< LOD	13.9	0.8	0.29
MSP 45	108.75	12.19	0.85	1.01	73.5	176.2	< LOD	393.8	< LOD	51.4	1.3	0.30
MSP 46	110.5	9.68	0.86	1.39	56.3	150.9	< LOD	454.2	< LOD	19.6	1.2	0.29
MSP 47	112.25	9.71	0.93	1.82	58.2	230.5	76.3	571.1	55.1	54.5	1.5	0.29
MSP 48	114	10.38	1.02	3.54	78.6	195.6	127.5	566.3	147.7	45.5	3.8	0.29
MSP 49	115.75	8.76	1.43	2.99	83.4	262.1	326.1	1177.5	150.1	55.4	3.1	0.37
MSP 50	117.5	10.93	1.00	1.57	71.7	185.1	< LOD	498.5	< LOD	< LOD	1.9	0.29

Table 1 continued
Geochemical data from McAlester Shale Pit, Oklahoma

Sample	Depth (ft) above Hunton	TOC (wt%)	Al (wt%)	Fe (wt%)	Mo (ppm)	U (ppm)	Mn (ppm)	V (ppm)	Ni (ppm)	Cu (ppm)	S (wt%)	P (wt%)
MSP 51	119.25	11.47	0.84	2.63	74.7	232.2	< LOD	428.3	25.8	15.2	2.7	0.28
MSP 52	121	9.98	0.58	4.07	73.9	141.8	54.0	305.9	47.2	52.5	1.8	0.30
MSP 53	122.75	10.36	1.10	2.48	91.9	214.3	65.3	551.1	< LOD	< LOD	3.1	0.30
MSP 54	124.5	11.09	1.09	3.52	99.3	170.6	81.9	422.0	42.6	27.9	4.3	0.28
MSP 55	126.25	14.70	1.13	3.45	101.1	219.1	72.6	389.2	< LOD	13.5	5.4	0.26
MSP 56	128	12.95	1.28	2.39	79.7	202.7	52.4	348.9	< LOD	< LOD	5.0	0.25
MSP 57	129.75	12.49	1.36	3.94	89.2	211.9	82.9	327.8	87.5	59.7	3.8	0.29
MSP 58	131.5	9.52	0.81	3.43	62.4	144.5	< LOD	236.9	< LOD	< LOD	3.5	0.28
MSP 59	133.25	11.44	1.26	2.72	88.8	246.7	338.6	327.3	43.8	33.2	2.2	0.29
MSP 60	135	13.51	0.76	2.48	57.9	251.4	73.0	310.3	< LOD	11.7	4.3	0.27
MSP 61	136.75	14.15	1.05	2.77	86.0	226.5	221.9	319.2	< LOD	32.5	2.5	0.31
MSP 62	138.5	11.50	1.35	3.22	62.6	211.1	269.5	392.2	49.7	31.7	2.6	0.32
MSP 63	140.25	12.56	1.18	3.69	82.3	182.1	168.0	310.2	43.0	37.3	3.6	0.33
MSP 64	142	15.49	1.34	4.27	112.0	211.8	108.9	328.6	36.5	35.3	4.4	0.28
MSP 65	143.75	11.82	1.24	2.87	82.2	216.7	197.7	347.5	71.6	31.0	2.7	0.35
MSP 66	145.5	12.68	1.12	2.89	83.3	238.6	164.7	355.1	89.2	34.2	2.7	0.36
MSP 67	147.25	12.62	1.26	2.62	83.7	195.7	43.5	383.2	< LOD	< LOD	2.9	0.37
MSP 68	149	9.78	1.21	3.19	63.4	242.5	388.1	308.8	73.2	32.1	2.0	0.36
MSP 69	150.75	10.54	1.42	3.21	74.0	265.3	307.1	356.9	89.2	28.6	2.8	0.35
MSP 70	152.5	12.16	1.35	2.96	88.9	213.8	82.6	383.0	43.8	19.0	3.0	0.37
MSP 71	154.25	12.50	1.59	3.46	80.3	247.5	140.8	408.1	102.2	37.6	3.3	0.36
MSP 72	156	12.62	1.05	2.02	89.8	161.5	< LOD	300.8	< LOD	< LOD	2.4	0.36
MSP 73	157.75	10.70	1.00	2.41	73.9	167.7	< LOD	314.6	< LOD	< LOD	2.5	0.41
MSP 74	159.5	11.36	1.31	3.48	71.8	209.1	46.6	333.5	< LOD	23.8	2.2	0.39
MSP 75	161.25	11.85	1.39	2.57	70.3	223.5	65.5	365.4	< LOD	< LOD	3.1	0.36
MSP 76	163	15.04	1.44	2.76	78.5	211.1	< LOD	409.4	< LOD	< LOD	3.8	0.35
MSP 77	164.75	12.39	2.01	4.60	87.9	428.7	510.2	473.6	235.6	51.5	2.1	0.37
MSP 78	166.5	16.78	1.40	2.20	85.2	250.5	< LOD	499.7	< LOD	< LOD	3.2	0.36
MSP 79	168.25	18.03	1.44	2.92	100.4	234.5	58.4	447.7	< LOD	< LOD	4.3	0.33
MSP 80	170	19.62	1.67	4.59	157.3	220.7	86.9	506.7	40.7	29.2	4.4	0.35
MSP 81	171.75	19.06	1.70	1.76	115.0	308.5	77.5	606.1	< LOD	< LOD	2.7	0.38
MSP 82	173.5	21.14	1.54	1.87	115.9	455.8	66.7	592.3	< LOD	< LOD	3.9	0.39
MSP 83	175.25	0.23	0.80	6.13	674.1	130.6	205.1	632.2	< LOD	68.3	< LOD	0.47
MSP 84	177	10.31	0.89	0.57	15.3	537.9	< LOD	320.0	< LOD	261.6	0.8	0.45

.

Table 2.
Geochemical data from Highway 77D, Oklahoma

Sample	Depth (ft) above Hunton	TOC (wt%)	Al (wt%)	Fe (wt%)	Mo (ppm)	U (ppm)	Mn (ppm)	V (ppm)	Ni (ppm)	Cu (ppm)	S (wt%)	P (wt%)
77D 01	0	0.84	3.34	1.74	< LOD	141.9	540.6	302.2	< LOD	79.7	0.0	< LOD
77D 02	2	0.07	3.57	1.54	< LOD	149.9	421.7	340.1	74.0	74.3	< LOD	< LOD
77D 03	4	1.51	5.23	1.97	6.6	447.9	46.7	1115.0	< LOD	171.0	0.1	0.8
77D 04	6	1.06	4.63	3.89	210.9	488.8	77.5	2006.5	< LOD	74.3	0.3	0.1
77D 05	8	20.72	2.28	2.99	330.3	263.9	< LOD	840.0	196.2	203.1	4.1	< LOD
77D 06	10	15.63	3.37	2.92	148.8	348.1	< LOD	921.2	154.2	200.5	2.9	0.1
77D 07	12	14.56	3.42	1.55	142.0	324.1	< LOD	1069.6	113.6	110.2	1.6	< LOD
77D 08	14	15.34	3.46	3.88	141.9	264.9	138.0	504.8	379.5	121.7	3.9	< LOD
77D 09	16	9.58	2.56	2.13	152.4	251.3	246.3	664.2	229.5	98.8	1.3	< LOD
77D 10	18	14.47	2.79	4.01	129.9	249.0	137.8	322.7	221.9	105.8	5.5	< LOD
77D 11	20	13.18	2.84	2.41	95.8	177.8	< LOD	349.1	90.0	74.1	3.5	< LOD
77D 12	22	15.43	2.75	2.58	14.0	145.8	114.8	271.5	94.0	146.1	11.5	< LOD
77D 13	24	0.65	2.09	7.61	239.5	170.1	300.4	1152.9	126.0	89.3	0.4	< LOD
77D 14	26	0.42	5.90	3.78	84.4	445.3	795.2	920.9	284.3	122.7	0.3	0.2
77D 15	28	2.24	3.64	3.93	176.2	634.0	54.7	971.8	46.7	164.9	0.2	< LOD
77D 16	30	9.46	4.39	2.84	88.7	392.1	227.1	715.4	252.9	102.8	2.6	< LOD
77D 17	32	13.12	2.92	1.61	84.7	190.0	160.9	449.6	246.1	99.0	2.3	< LOD
77D 18	34	15.86	2.47	2.58	165.7	409.4	< LOD	397.2	99.6	127.9	4.3	< LOD
77D 19	36	17.64	2.94	1.33	184.4	274.9	< LOD	481.9	68.1	57.9	2.9	< LOD
77D 20	38	9.59	2.08	1.26	96.5	207.3	< LOD	278.3	< LOD	28.1	2.0	< LOD
77D 21	40	13.40	2.85	1.84	111.8	279.4	< LOD	330.5	< LOD	31.8	2.6	0.1
77D 22	42	13.58	2.25	1.94	170.7	318.1	< LOD	352.2	< LOD	121.0	2.5	0.1
77D 23	44	13.16	2.72	0.86	122.8	260.5	< LOD	298.5	< LOD	54.7	1.9	0.1
77D 24	46	8.53	2.69	1.69	89.4	277.4	< LOD	322.2	< LOD	58.4	2.1	0.1
77D 25	48	10.60	3.04	1.68	116.0	269.2	< LOD	357.8	< LOD	31.2	3.2	0.2
77D 26	50	5.33	3.53	2.62	178.7	356.7	64.1	425.9	< LOD	105.0	0.6	0.2
77D 27	52	8.67	2.62	2.26	28.7	202.4	306.4	295.1	< LOD	53.2	2.3	0.2
77D 28	54	9.02	3.01	2.44	47.5	210.8	261.0	334.2	27.3	64.0	3.1	0.2
77D 29	56	0.00	no data	no data	no data	no data	no data	no data	no data	no data	no data	no data
77D 30	58	8.92	3.84	2.04	77.9	356.5	168.6	548.9	117.3	85.8	2.0	0.2
77D 31	60	12.53	2.62	2.09	178.4	337.9	< LOD	451.8	48.8	85.0	3.0	0.2
77D 32	62	0.00	no data	no data	no data	no data	no data	no data	no data	no data	no data	no data
77D 33	64	3.92	1.41	1.52	14.8	77.6	217.8	198.9	< LOD	15.7	1.2	0.3
77D 34	66	10.41	3.39	2.19	99.1	296.1	94.6	464.0	118.0	90.0	3.2	0.2
77D 35	68	12.76	3.16	4.18	165.3	354.9	84.7	513.0	116.6	106.6	4.3	0.2
77D 36	70	4.76	2.92	2.52	141.7	370.5	47.2	531.7	< LOD	110.4	1.1	0.3
77D 37	72	5.66	2.96	3.34	77.2	265.1	59.8	447.6	42.1	90.6	1.4	0.3

Table 3
Metal/Al ratios in the Post-Archean Average
Shale standard (PAAS; Tayor and McCennan, 1985)

	Metal/Al
wt.%/wt.%	
Fe	0.51
P	0.01
ppm/wt.%	
Mo	0.1
U	0.31
Mn	89.98
V	15
Ni	5.5
Cu	5

.

VITA

Robert Riter Berryman

Candidate for the Degree of

Master of Science

Thesis: CONSTRAINTS ON DEVELOPMENT OF ANOXIA THROUGH GEOCHEMICAL FACIES MAPPING OF DEVONIAN BLACK SHALES IN THE MIDCONTINENT

Major Field: Petroleum Geology

Biographical:

Education:

Completed the requirements for the Master's of Science in Geology at Oklahoma State University, Stillwater, Oklahoma in May, 2012.
Completed the requirements for the Bachelor of Science in Geology at Oklahoma State University, Stillwater, OK in 2008.

Experience:

Geologist, Samson Resources, Tulsa OK, June, 2012
Geology Intern at Noble Energy, Denver CO, summer 2011

Professional Memberships:

American Association of Petroleum Geologist
Geological Society of America
Oklahoma State University Geological Society
Tulsa Geological Society

Name: Robert Riter Berryman Date of Degree: May, 2012

Institution: Oklahoma State University Location: Stillwater, Oklahoma

Title of Study: CONSTRAINTS ON DEVELOPMENT OF ANOXIA THROUGH GEOCHEMICAL FACIES MAPPING OF DEVONIAN BLACK SHALES IN THE MIDCONTINENT

Pages in Study: 66 Candidate for the Degree of Master of Science

Major Field: Petroleum Geology

Scope and Method of Study:

To examine the cause of anoxic conditions in the Woodford Shale, an integrated lithologic-geochemical study of several outcrops located in south-central Oklahoma was implemented. Trace metal concentrations were measured using a hand-held XRF instrument, with TOC concentrations measured in the laboratory.

Findings and Conclusions:

The Woodford Shale of the US southern Midcontinent is an Upper Devonian/Lower Mississippian black shale sequence that includes the Frasnian-Famennian boundary. Black shales are commonly enriched in transition metals. While the details of the chemical reactions and feedbacks responsible for trace metal enrichment are debated, these elements continue to be valuable for constraining paleoenvironmental conditions and potential source rock characteristics. While anoxic conditions are thought to favor the preservation of high concentrations of trace metals and total organic carbon (TOC), debate continues concerning the specific role of anoxia in the preservation of TOC, as well as the importance of eustatic sea-level shifts in the development of anoxia during Woodford Shale deposition—and by extension in other shale gas units.

Metal/TOC ratios vary systematically with depth in these units within single outcrop, providing constraints on the role of bottom-water restriction in the development of these shales. Geographic variations in the concentrations of proxies for anoxia (i.e., higher trace metal concentrations at outcrops interpreted to be further from shore), TOC concentrations and shale lithologies provide evidence for a key role played by water-column productivity in the development of anoxia.

Geochemical analysis of TOC concentrations and trace element ratios from Woodford Shale outcrops located at the McAlister Shale Pit in Carter County and at Highway 77D in Murray County in south-central Oklahoma, allowed for the placement of the two Woodford Shale outcrops onto an inferred depositional model. In this refined model, the 77D outcrop is located more proximal to the shoreline, in shallower waters, than the McAlister Shale Pit. Higher metal/Al ratios together with higher TOC concentrations are interpreted to indicate that the McAlister Shale Pit was located in generally deeper waters relative to 77D.

ADVISER'S APPROVAL: Dr. Jim Puckette